Positron emission tomography imaging of prostate cancer

Hao Hong[1], **Yin Zhang**[1], **Jiangtao Sun**[1], and **Weibo Cai**[1,2]

[1]Departments of Radiology and Medical Physics, School of Medicine and Public Health, University of Wisconsin - Madison, Madison, Wisconsin, USA

[2]University of Wisconsin Carbone Comprehensive Cancer Center, Madison, Wisconsin, USA

Abstract

Prostate cancer (PCa) is the second leading cause of cancer death among men in the United States. Positron emission tomography (PET), a non-invasive, sensitive, and quantitative imaging technique, can facilitate personalized management of PCa patients. There are two critical needs for PET imaging of PCa, early detection of primary lesions and accurate imaging of PCa bone metastasis, the predominant cause of death in PCa. Since the most widely used PET tracer in the clinic, ^{18}F-fluoro-2-deoxy-2-D-glucose (^{18}F-FDG), does not meet these needs, a wide variety of PET tracers have been developed for PCa imaging which span an enormous size range from small molecules to intact antibodies. In this review, we will first summarize small molecule-based PET tracers for PCa imaging, which measure certain biological events such as cell membrane metabolism, fatty acid synthesis, and receptor expression. Next, we will discuss radiolabeled amino acid derivatives (e.g. methionine, leucine, tryptophan, and cysteine analogs), which are primarily based on the increased amino acid transport of PCa cells. Peptide-based tracers for PET imaging of PCa, mostly based on the bombesin peptide and its derivatives which bind to the gastrin-releasing peptide receptor, will then be presented in detail. We will also cover radiolabeled antibodies and antibody fragments (e.g. diabodies and minibodies) for PET imaging of PCa, targeting integrin $\alpha_v\beta_3$, EphA2, the epidermal growth factor receptor, or the prostate stem cell antigen. Lastly, we will identify future directions for the development of novel PET tracers for PCa imaging, which may eventually lead to personalized management of PCa patients.

Keywords

Molecular imaging; prostate cancer; positron emission tomography (PET); peptide; antibody

Introduction

Prostate cancer (PCa) is the second leading cause of cancer death among men in the United States, with an estimated 186,320 new cases and 28,660 deaths in 2008 (Jemal et al. 2008). When diagnosed early, the 5-year survival rate of PCa is almost 100%. However, although hormonal treatment of PCa metastases is initially successful with response rates of more than 90%, hormone refractory disease will usually develop after about 18–24 months (Eisenberger et al. 1998). Therefore, accurate localization of the tumor as well as whole body burden determination of PCa is critically important for selecting the most effective treatment, with the goal of improving cancer control while reducing the risk of intervention-related complications.

Requests for reprints: Weibo Cai, PhD, Departments of Radiology and Medical Physics, School of Medicine and Public Health, University of Wisconsin - Madison, 1111 Highland Ave, Room 7137, Madison, WI 53705-2275, USA., Tel: 608-262-1749, Fax: 608-265-0614, wcai@uwhealth.org.

Current clinical diagnostic methods for localizing PCa adopt both the conventional anatomic imaging techniques, such as computed tomography (CT) (Hricak et al. 2007; Price and Davidson 1979), ultrasound (Cury et al. 2006; Fuchsjager et al. 2008; Linden and Halpern 2007), and magnetic resonance imaging (MRI) (Rorvik and Haukaas 2001), and molecular imaging techniques such as magnetic resonance spectroscopy (Kurhanewicz et al. 2008; Mueller-Lisse et al. 2007; Squillaci et al. 2005), single-photon emission computed tomography (SPECT) (Ananias et al. 2008; Reubi and Maecke 2008; Seo et al. 2006) and positron emission tomography (PET) (Bouchelouche and Oehr 2008; Emonds et al. 2009; Farsad et al. 2008; Larson and Schoder 2008). The conventional imaging techniques have played a rather limited role in the diagnosis, staging, and monitoring of PCa patients because PCa can be indistinguishable from the surrounding normal prostate tissue (Norberg et al. 1997). Molecular imaging techniques can provide more biologically relevant information that is necessary for understanding the tumor physiology, thereby enabling more accurate prognosis and therapeutic monitoring.

Among all molecular imaging techniques, PET is the most sensitive and has been applied in the diagnosis of PCa. Based on the use of positron-emitting radioisotopes, PET imaging can provide non-invasive and, more importantly, quantitative images of the tracer in intact living subjects (i.e. animals for pre-clinical studies and humans for clinical studies, respectively) (Gambhir 2002; Phelps 2000). The two critical needs for PET imaging of PCa are early detection of primary lesions and accurate localization of PCa bone metastasis. In this review, we will first briefly introduce the commonly used PET tracers for PCa imaging. Then, we will focus on peptide-based tracers which range from a single amino acid to macromolecules such as antibodies. Knowledge of both the benefits and disadvantages of these PET tracers will help the clinicians to make the right decision in both diagnosis and management of PCa.

Small molecule-based PET tracers for PCa imaging

The most commonly used and most successful PET tracer for cancer diagnosis is ^{18}F-fluoro-2-deoxy-2-D-glucose (^{18}F-FDG, Fig. 1) (Gambhir et al. 2001). Tumor imaging with ^{18}F-FDG is based on the fact that cancer cells are more metabolically active than normal cells. Most cancer cells actively take up and transport ^{18}F-FDG into glycolysis, where it is phosphorylated to ^{18}F-FDG-6-phosphate by hexokinase (Pauwels et al. 1998). ^{18}F-FDG-6-phosphate is then trapped inside the cells which gives PET contrast of the tumor tissue. ^{18}F-FDG uptake in PCa was reported to correlate with the prostate-specific antigen (PSA) level, thus it can be used as a measure of tumor aggressiveness (Seltzer et al. 1999). ^{18}F-FDG PET can also be useful in monitoring the therapeutic responses of patients with aggressive or hormone refractory diseases (Morris et al. 2005;Morris et al. 2002). However, generally speaking, ^{18}F-FDG PET imaging in PCa has not been very successful due to several reasons. First, glucose utilization in well-differentiated PCa is often lower than in other tumor types, which leads to low tumor uptake of ^{18}F-FDG and poor image contrast. Second, the intense accumulation of ^{18}F-FDG in the urinary bladder, which is in close proximity to the prostate, often overshadows the tumor uptake (Mathews and Oz 2002). Third, no correlation was observed between tumor grade/stage and the ^{18}F-FDG uptake in PCa (Effert et al. 1996). In one study, it was reported that when compared with CT, ultrasound, or MRI, ^{18}F-FDG PET of PCa did not reveal any additional information (Effert et al. 1996).

Due to the limitations of ^{18}F-FDG PET, several other small molecule-based tracers were developed and evaluated for PET imaging of PCa which include: ^{11}C- or ^{18}F-labeled choline analogs (imaging of cell membrane metabolism) (de Jong et al. 2002; DeGrado et al. 2007; Farsad et al. 2005; Hara et al. 2002; Husarik et al. 2008), ^{18}F-fluoride (imaging of osteoblastic activity) (Beheshti et al. 2008), ^{18}F- or ^{11}C-acetate (imaging of fatty acid synthesis) (Albrecht et al. 2007; Nanni et al. 2007; Ponde et al. 2007; Vavere et al. 2008), ^{64}Cu-diacetyl-bis(N^4-

methylthiosemicarbazone (^{64}Cu-ATSM, imaging of hypoxia) (Vavere and Lewis 2008), and ^{18}F-3'-deoxy-3'-fluorothymidine (^{18}F-FLT, imaging of proliferation) (Bouchelouche and Oehr 2008; Oyama et al. 2004) (Fig. 1). In various clinical or experimental scenarios, these tracers exhibited certain advantages over ^{18}F-FDG such as reduced urinary excretion, better sensitivity and diagnostic accuracy, as well as more insight into the pathobiological characteristics of PCa. However, these tracers are not PCa specific. In some cases, inefficient radiolabeling and synthesis methods have also limited the applications of certain PET tracers for widespread clinical use in the future.

The development of PET tracers that can be targeted to specific molecular markers over-expressed in PCa is crucial for the accurate diagnosis of PCa. The normal development and maintenance of the prostate is dependent on androgen acting through the androgen receptor (AR), which remains important in the development and progression of PCa (Heinlein and Chang 2004). Since AR is activated by binding of either of the androgenic hormones, testosterone or dihydrotestosterone, ^{18}F-fluoro-5α-dihydrotestosterone (^{18}F-FDHT, Fig. 1) was developed for PET imaging of PCa (Dehdashti et al. 2005; Larson et al. 2004; Zanzonico et al. 2004). ^{18}F-FDHT appears to be useful in evaluating clinically progressive metastatic PCa and may be a promising agent in measuring tumor responses to treatment. However, this tracer is not very useful in androgen-independent PCa since the tracer uptake may not be relevant to PCa development in these cases.

Peptides and their derivatives are of particular interest for PET tracer development because they have many favorable characteristics including fast clearance from the circulation, rapid tissue penetration, and low antigenicity. There has been a tremendous growth in the development of radiolabeled peptides for diagnostic and therapeutic applications in the last decade (Weiner and Thakur 2005). The easy and automated means of synthesizing these compounds, along with simplified methods for purification, characterization, and optimization of peptides, make them highly attractive targeting molecules (Lebl and Hachmann 2005; Reader 2004). A variety of PET tracers have been developed for targeting either universal or PCa specific antigens/receptors, including the prostate-specific membrane antigen (PSMA), prostate stem cell antigen (PSCA), gastrin-releasing peptide receptor (GRPR), integrin $α_v β_3$, among others. The targeting ligands used in these tracers span the wide range from single amino acids to peptides to antibodies, which is the main focus of this review.

Radiolabeled amino acid derivatives for PET imaging of PCa

PET imaging of tumor cell metabolism has been very successful over the last decade. Numerous studies have demonstrated that tumors can be detected with high sensitivity and specificity by imaging their increased metabolic rates for glucose (with ^{18}F-FDG) or lipids (with radiolabeled choline analogs) (Plathow and Weber 2008). Another important area for imaging tumor cell metabolism is the amino acid transport. A number of amino acid derivatives have been radiolabeled for PET imaging of cancer, with the most popular ones being [N-methyl-^{11}C]α-methylaminoisobutyric acid (^{11}C-MeAIB, Fig. 2) (Sutinen et al. 2001; Tolvanen et al. 2006), and radiolabeled methionine/tyrosine/phenylalanine analogs (Laverman et al. 2002; McConathy and Goodman 2008; Plathow and Weber 2008). Here we will only focus on the radiolabeled amino acid derivatives that have been tested for PET imaging of PCa.

^{11}C-methionine

One of the earliest investigated amino acid-based PET tracers for PCa imaging is ^{11}C-methionine (Fig. 2) (Larson and Schoder 2008;Macapinlac et al. 1999;Toth et al. 2005). Uptake of ^{11}Cmethionine is related to amino acid transport and protein synthesis, which is indicative of active tumor proliferation. Methionine is rapidly cleared from the blood and is metabolized in both the liver and the pancreas without renal excretion, which makes it more suitable

than ^{18}F-FDG for imaging pelvic malignancies such as PCa. In 1999, the pharmacokinetics of ^{11}C-methionine was compared with ^{18}F-FDG in a group of androgen-independent, metastatic PCa patients to determine the optimal time of imaging after tracer injection (Macapinlac et al. 1999). The plateau of ^{11}C-methionine uptake in the tumor was reached within 10 minutes, and thereafter remained constant. Tumor uptake of ^{18}F-FDG was slower, and for some patients it continued to rise beyond 45 minutes. The clearance of blood activity for ^{11}C-methionine was more rapid than ^{18}F-FDG and the standardized uptake value (SUV) of ^{11}C-methionine was also significantly higher than that of ^{18}F-FDG. The major advantages of ^{11}C-methionine over ^{18}F-FDG are higher tumor-to-blood ratio, more rapid tumor uptake which allows earlier imaging, and a flatter plateau which makes lesion activity on whole body images more uniform and less susceptible to gradual changes.

A subsequent study confirmed these advantages of ^{11}C-methionine over ^{18}F-FDG (Nunez et al. 2002), and further revealed that ^{11}C-methionine was more effective for detecting bone metastasis in PCa patients. In 2005, ^{11}C-methionine PET was carried out in a rising-PSA population with negative findings on repeated biopsies (Toth et al. 2005). With an overall detection rate of 46.7% (7/15), ^{11}C-methionine PET of the prostate with short dynamic scans, in combination with multicore biopsy, was found to be useful for ensuring a high detection rate of PCa in the patient population investigated in this study.

Besides the frequently used ^{11}C-methionine, many other radiolabeled amino acid derivatives have been developed for PET imaging of PCa (Fig. 2), such as 1-aminocyclobutane-^{11}C-carboxylic acid (^{11}C-ACBC) (Hubner et al. 1981), anti-1-amino-3-^{18}F-fluorocyclobutyl-1-carboxylic acid (anti-^{18}F-FACBC) (Nye et al. 2007;Oka et al. 2007;Schuster et al. 2007), ^{11}C-5-hydroxytryptophan (^{11}C-5-HTP) (Kalkner et al. 1997), N-[N-[(S)-1,3-dicarboxypropyl]carbamoyl]-S-[^{11}C]methyl-L-cysteine (^{11}C-DCMC) (Foss et al. 2005), and N-[N-[(S)-1,3-dicarboxypropyl]carbamoyl]-4-[^{18}F]fluorobenzyl-L-cysteine (^{18}F-DCFBC) (Mease et al. 2008). Three main mechanisms apply to those PET tracers: amino acids transport (^{11}C-ACBC and anti-^{18}F-FACBC), neuroendocrine tumor targeting (^{11}C-5-HTP), and PSMA targeting (^{11}C-DCMC and ^{18}F-DCFBC).

Radiolabeled leucine analogs

^{11}C-ACBC, a radiolabeled L-leucine analog, was developed for PET imaging almost three decades ago (Hubner et al. 1981). This tracer exhibited good tumor-to-normal tissue (T/N) ratio, little renal excretion, and high pancreatic uptake. More than a decade later, an automated radiosynthesis of ^{11}C-ACBC was reported (Goodman MM 1994). Although ^{11}C-ACBC was demonstrated useful for cancer detection, the short decay half-life of ^{11}C (~ 20 minutes) is the major drawback for its clinical use. Therefore, an ^{18}F-labeled ACBC analog, in which ^{18}F replaces a hydrogen atom (i.e. anti-^{18}F-FACBC), was synthesized and tested for brain tumor imaging (Shoup et al. 1999). Anti-^{18}F-FACBC has similar imaging characteristics as ^{11}C-ACBC. However, the significantly longer decay half-life of about 110 minutes allows sufficient time for incorporation of ^{18}F into the PET tracer. More importantly, multiple doses can be generated from a single-batch of ^{18}F-labeling, more practical PET imaging protocols can be implemented, and regional shipment of the tracer to satellite facilities with PET scanners is also possible.

In 2007, the potential use of anti-^{18}F-FACBC in PCa diagnosis was evaluated in a rat orthotopic PCa model (Oka et al. 2007). Biodistribution studies at 1 hour after tracer injection showed that uptake of anti-^{18}F-FACBC in the PCa tissue was comparable to that of ^{18}F-FDG. However, the accumulation of anti-^{18}F-FACBC in the urinary bladder was more than 20 fold lower than that of ^{18}F-FDG. Thus, PET imaging with anti-^{18}F-FACBC had significantly better tumor contrast than ^{18}F-FDG PET, which facilitated the visualization of PCa tissue in these rats.

Further, higher ratios of PCa-to-inflammation and PCa-to-benign prostatic hyperplasia (BPH) were also observed for anti-^{18}F-FACBC than ^{18}F-FDG.

Subsequently, the diagnostic efficiency of anti-^{18}F-FACBC PET in PCa patients was studied (Nye et al. 2007; Schuster et al. 2007). Patients with a recent diagnosis of PCa (n = 9) or suspected recurrence (n = 6) underwent 65-minute dynamic PET/CT scans of the pelvis after intravenous injection of anti-^{18}F-FACBC, followed by static PET/CT scans (Schuster et al. 2007). It was found that pelvic nodal status correlated with anti-^{18}F-FACBC PET findings in 7 of the 9 patients (77.8%). In all 4 patients with proven recurrence, visual analysis of the PET images was able to identify the PCa lesions. In contrast, ^{111}In-capromab-pendetide, a radiolabeled anti-PSMA antibody widely used for PCa diagnosis with SPECT (Manyak 2008; Sodee et al. 2005), had no significant uptake in either the nodal or the skeletal foci in 3 of the 4 patients (Fig. 3). Although the tumor uptake dropped over time, intense and persistent uptake of anti-^{18}F-FACBC was observed at 65 minutes post-injection in all 6 patients with either lymph node metastases or recurrent prostate bed carcinoma. Dosimetry studies indicated that injection of 370 MBq (i.e. 10 mCi) of anti-^{18}F-FACBC could give both good PET image quality and acceptable dosimetry (Nye et al. 2007).

In a recent case study, anti-^{18}F-FACBC PET was evaluated for its potential in assisting radiotherapy planning of a PCa patient (Jani et al. 2009). Although more patients will be needed to further validate the results, this pilot study did demonstrate the feasibility of anti-^{18}F-FACBC PET in guiding radiotherapy of PCa patients. In general, these ACBC-based PET tracers exhibited the following characteristics: high uptake in the PCa tissue but not in the normal prostate and BPH, low uptake in inflammatory tissues, and minimal renal excretion which results in low radioactivity in the bladder. These favorable properties warrant further clinical investigation of radiolabeled leucine analogs in PCa patients, in particular ^{18}F-FACBC.

Radiolabeled tryptophan analog

The discovery of neuroendocrine differentiation in hormone refractory PCa has opened a potentially new therapeutic approach for this group of patients, where very few effective therapies are available (Kalkner et al. 1997). Based on previous findings of increased uptake of ^{11}C-5-HTP in neuroendocrine tumors (Eriksson et al. 1993), this tracer was tested in a study of metastatic hormone refractory PCa (Kalkner et al. 1997). Uptake of ^{11}C-5-HTP was observed in all investigated skeletal lesions, however the magnitude of the uptake was moderate. Although the difference between the SUV in normal bone and metastatic lesions was statistically significant, the SUV varied between patients, as well as between lesions over time and treatment. Nonetheless, the ability of ^{11}C-5-HTP in discriminating metastatic lesions from normal bone may aid in the diagnosis and, potentially, treatment monitoring of metastatic hormone refractory PCa.

Radiolabeled cysteine analogs

PSMA is expressed in almost all PCa cells, from primary to metastatic lesions, and appears to be maximally expressed after androgen withdrawal (Chang et al. 1999; Silver et al. 1997; Sweat et al. 1998). Imaging agents such as radiolabeled antibodies which target the PSMA can localize to the tumor and thereby distinguish non-cancer-related abnormalities from malignant lesions (Hinkle et al. 1998; Texter and Neal 1998). However, the long circulation life-time of radiolabeled antibodies (usually several days) can affect the T/N ratio because of significant background signal. Therefore, peptide- and/or amino acid-based PSMA targeting molecules are attractive alternatives for PET imaging of PCa.

PET imaging of xenografted tumors that over-express the PSMA was successfully achieved with an ^{11}C-labeled PSMA inhibitor, ^{11}C-DCMC, which was reported to bind to the

extracellular active site of PSMA (Foss et al. 2005). At 30 minutes post-injection, ^{11}C-DCMC showed tumor-to-muscle ratios of about 10 with clear delineation of the tumor. Recently, the same PSMA inhibitor was labeled with [18]F (Mease et al. 2008). Mice bearing both subcutaneous PSMA-positive and PSMA-negative tumors were injected with ^{18}F-DCFBC for both ex vivo biodistribution studies and PET imaging applications. Both experiments showed high uptake of ^{18}F-DCFBC in the PSMA-positive tumors with little to no uptake in the PSMA-negative tumors (Fig. 4). High radioactivity was also seen in the kidneys and bladder, due to the renal excretion of ^{18}F-DCFBC, however the washout of radioactivity from these organs was faster than from the PSMA-positive tumors. These results confirmed that[18]F-DCFBC localized to PSMA-positive tumors in mice, permitting non-invasive imaging of PCa with small-animal PET which makes it an attractive candidate for further clinical investigation.

Generally speaking, radiolabeled amino acids or their derivatives can be superior to [18]FFDG and/or radiolabeled antibodies for imaging primary PCa. However, much further optimization and clinical investigation will be needed before these PET tracers can make a significant impact on the management of PCa patients. With the exception of the PSMA-targeting tracers (i.e. ^{11}C-DCMC and ^{18}F-DCFBC), the abovementioned PET tracers are not PCa specific since they take advantage of the fact that most tumors have elevated protein synthesis rate which requires increased amino acid transport. Such processes occur in almost all cancer types, not only in PCa. More specific PET tracers need to be developed for imaging PCa-related molecular and/or cellular events. In the next section, we will describe the use of peptide-based PET tracers for PCa imaging.

Radiolabeled peptides for PCa imaging

Radiolabeled peptides have been widely investigated for PET imaging of various types of cancer and tremendous progress has been made over the last decade. A classic example is radiolabeled Arg-Gly-Asp (RGD) peptides and their derivatives for imaging tumor expression of integrin $\alpha_v\beta_3$, a cell adhesion molecule which plays important roles during tumor angiogenesis and metastasis (Cai and Chen 2006; Cai et al. 2008a). ^{18}F-labeled RGD peptides have entered phase I clinical trials in many cancer types and been proven to be safe, metabolically stable, and retained in the tumor tissue (Cai et al. 2008a). Many other peptides have also been investigated for cancer imaging, such as somatostatin analogs (e.g. octreotide and pentetreotide which are well-studied for the imaging of neuroendocrine tumors) (Froidevaux and Eberle 2002; Lewis and Anderson 2007), minigastrin (which targets the cholecystokinin-2 receptors) (Reubi 2007; Reubi and Maecke 2008), neuropeptide-Y analogs (Zwanziger et al. 2008), among others.

Despite the success achieved by the abovementioned radiolabeled peptides, their applications in PCa imaging have not been satisfactory, largely due to the many characteristics of primary PCa such as comparatively low metabolism and different receptor expression level (Agrawal et al. 2009; Apolo et al. 2008; Bouchelouche and Oehr 2008). For example, ^{18}F-labeled RGD peptides (including multimeric RGD peptides which have high affinity for integrin $\alpha_v\beta_3$) had only moderate uptake in the PCa tumors, presumably because of the insufficient expression level of integrin $\alpha_v\beta_3$ in the PCa tissue (Zhang et al. 2006b). Therefore, choosing the right molecular targets which are expressed at high levels in the PCa tissue is critical to the success of peptide-based imaging of PCa. Currently, the most popular candidates are the bombesin (BBN) peptides and their derivatives which can bind to the GRPR (Ananias et al. 2008).

GRPR is a glycosylated, 7-transmembrane G protein-coupled receptor in mammals (Ananias et al. 2008; Cornelio et al. 2007). Studies have shown that it is massively over-expressed in several human tumors, in particular breast cancer and PCa (Gugger and Reubi 1999; Markwalder and Reubi 1999). On the other hand, GRPR expression in benign prostate tissues

ranges from low to non-detectable (Bartholdi et al. 1998; Markwalder and Reubi 1999), which makes it an attractive target for PCa imaging. Various approaches have been explored for imaging GRPR expression in vivo. Gastrin-releasing peptide (GRP) binds to GRPR with high affinity, however BBN peptide (originally isolated from the skin of a type of frog) is typically used for imaging applications (Ananias et al. 2008). The BBN peptide, consisting of 14 amino acids (Fig. 5a), was first reported in 1970 (Erspamer et al. 1970). The GRP and BBN peptides share an identical C-terminal region, consisting of 7 amino acids, which is necessary for GRPR binding (McDonald et al. 1979). Therefore, the truncated sequence, BBN(7–14) (Fig. 5b), was also often used for imaging applications.

Most BBN derivatives are agonists for GRPR, which are internalized after receptor binding. It is generally believed that tumor uptake of an agonist-based tracer will be higher than that of an antagonist-based tracer (which does not get internalized), because the agonist-based tracer can be trapped inside the cell. However, the binding affinity of the ligand to the receptor also plays a critical role, and tumor cell uptake of antagonists can be much higher because of its stronger binding to the receptor (Cescato et al. 2008). Further studies need to be carried out to determine which factor is more important for the tumor targeting efficacy, since internalization is just one of the many factors that can affect the tumor cell uptake of the tracer. BBN derivatives have mainly been labeled with three isotopes for PET imaging of PCa: ^{64}Cu (half-life: 12.7 hours), ^{18}F, and ^{68}Ga (half-life: 68 minutes).

^{64}Cu-labeled BBN analogs

^{64}Cu-labeled BBN derivatives, both the full length BBN peptide and its truncated form, have been reported. In an early study, the potential of ^{64}Cu-DOTA-Aoc-BBN(7–14) (DOTA denotes 1,4,7,10-tetraazacyclododecane-1,4,7,10-tetraacetic acid and Aoc denotes aminooctanoic acid, respectively) for PET imaging of GRPR-positive PCa was investigated (Rogers et al. 2003). This tracer exhibited rapid internalization into PCa cells, as well as good tumor localization capability in vivo. However, uptake of the tracer in the liver, kidneys, pancreas, and intestine was also high, resulting in a low T/N ratio. Although an excess amount of unlabeled BBN peptide could block the tracer uptake in the PCa tumor and the pancreas, which confirmed GRPR specificity of the tracer in these tissues in vivo, uptake in the liver was not blocked which was likely due to transchelation of ^{64}Cu to other proteins such as albumin (Rogers et al. 1996).

One study investigated the importance of various aliphatic linkers between the BBN analog and the DOTA chelator to the imaging characteristics of the tracer (Parry et al. 2007). It was concluded that the use of amino acid linkers (combinations of glycine, serine, and/or glutamic acid) between the DOTA chelator and the BBN analog could reduce non-specific tissue uptake, while maintaining good PCa uptake of the tracer. The same BBN(7–14) peptide has been labeled with ^{64}Cu using a different chelator, NOTA (1,4,7-triazacyclononane-1,4,7-triacetic acid), in order to improve the T/N ratio (Prasanphanich et al. 2007). In vivo studies of ^{64}Cu-NOTA-Aoc-BBN(7–14) in PC-3 mouse models indicated very high affinity of the tracer for GRPR. Further, minimal accumulation of radioactivity in the liver (1.6 ± 0.4 percentage injected dose per gram of tissue [%ID/g] at 1 hour post-injection) suggested rapid renal excretion and excellent in vivo stability of this tracer, with little dissociation of ^{64}Cu from the NOTA chelator in vivo. Such effect was then explored with another chelator for ^{64}Cu-labeling, CB-TE2A (1,4,8,11-tetrazazbicyclo[6.6.2]hexadecane-4,11-diacetic acid) (Garrison et al. 2007). The further improved T/N ratio and significantly faster clearance of the tracer confirmed that the choice of the chelator is important for successful PET imaging with ^{64}Cu-labeled BBN analogs. Recently, another chelator, 2-[4,7-bis(2-pyridylmethyl)-1,4,7-triazacyclononan-1-yl] acetic acid, was also reported for ^{64}Cu-labeling (Gasser et al. 2008). However, no in vivo imaging data is available yet.

All the abovementioned tracers were based on truncated BBN rather than the complete sequence. In 2004, ^{64}Cu-labeled [Lys^3]BBN, the complete sequence with all 14 amino acid residues, was reported for PET imaging of GRPR expression in PCa models (Chen et al. 2004). Tissue biodistribution, small-animal PET, and whole body autoradiography studies of the tracer were investigated in both the androgen-independent PC-3 and androgen-dependent CRW22 tumors. It was found that PC-3 tumor uptake of the tracer (5.6 ± 0.1 %ID/g at 30 minutes post-injection) was more than 3-fold higher than that of the CWR22 tumor (1.8 ± 0.1 %ID/g), which appeared to be mostly non-specific. Significant accumulation of radioactivity in the pancreas (GRPR-positive) was also observed. PET imaging, after intravenous injection of ^{64}Cu-DOTA-[Lys^3]BBN, of mice bearing both subcutaneous PC-3 and CWR22 tumors exhibited good T/N contrast, which was confirmed by autoradiography (Fig. 6a).

To investigate whether the C-terminal truncated form of BBN (i.e. BBN(7–14)) or the full-length version is more suitable for GRPR targeting in vivo, the receptor binding affinity, metabolic stability, tumor-targeting efficacy, and pharmacokinetics of ^{64}Cu-DOTA-Aca-BBN (7–14) were compared with ^{64}Cu-DOTA-[Lys3]BBN in a follow-up study (Yang et al. 2006). It was found that the full-length BBN had higher GRPR affinity in vitro, better metabolic stability, superior tumor contrast, as well as more prominent tumor uptake in vivo. In another report, DOTA-[Pro^1,Tyr^4]BBN was investigated for PET imaging of PCa with both ^{64}Cu and ^{86}Y (Biddlecombe et al. 2007). Interestingly, the ^{86}Y-labeled peptide exhibited better PET image quality in all the PCa models tested in this study for the delineation of GRPR-positive tumors. This finding deserves further investigation.

^{18}F-labeled BBN analogs

Being the most widely used radionuclide for PET, ^{18}F is the ideal isotope for labeling small biologically active peptides (Okarvi 2001). Over the last decade, a number of prosthetic groups have been explored for ^{18}F-labeling of peptides (Cai et al. 2008a). In one study, both [Lys^3] BBN and Aca-BBN(7–14) were labeled with ^{18}F (Zhang et al. 2006a). These tracers showed rapid internalization into PC-3 cells. However, a rapid efflux of both tracers also occurred, which is quite different from the ^{64}Cu-labeled BBN analogs. Both tracers exhibited rapid blood clearance and the ^{18}F-labeled [Lys^3]BBN had predominant renal excretion while the ^{18}F-labeled Aca-BBN(7–14) exhibited both hepatobiliary and renal clearance. Dynamic small-animal PET imaging studies revealed that the PC-3 tumor uptake of ^{18}F-labeled [Lys^3]BBN was much higher than that of ^{18}F-labeled Aca-BBN(7–14) at all time points examined. More importantly, the ^{18}F-18 labeled [Lys^3]BBN was also able to visualize orthotopic PC-3 tumor at early time points (between 10 and 30 minutes) after tracer administration, during which minimal urinary bladder radioactivity was present to interfere with the receptor-mediated tumor uptake.

Recently, a dual-receptor targeting heterodimer, formed by linking a GRPR targeting ligand and an integrin $\alpha_v\beta_3$ targeting ligand, was synthesized to increase the PCa tumor uptake and T/N ratios (Li et al. 2008). It was hypothesized that because of its dual-receptor targeting capability, a tracer recognizing both GRPR and integrin $\alpha_v\beta_3$ will be more advantageous than the tracers based on either ligand alone. The BBN-RGD heterodimer was synthesized from BBN(7–14) and c(RGDyK) with a glutamate linker, which was then labeled with ^{18}F (Li et al. 2008). The ^{18}F-labeled heterodimer, ^{18}F-FB-BBN-RGD, had comparable integrin $\alpha_v\beta_3$-binding affinity with c(RGDyK) and similar GRPR-binding affinity as BBN(7–14). In vivo, ^{18}F-FB-BBN-RGD had significantly higher PC-3 tumor uptake, as well as better PET image quality, than both the monomeric RGD-based and monomeric BBN(7–14)-based tracers (Fig. 6b). However, there are two major limitations of this study: first, two products were formed during the synthesis of the heterodimer (i.e. BBN-RGD and RGD-BBN) which were

not separable; Second, the radiolabeling yield was quite low, presumably due to the steric hindrance.

To overcome these limitations, the researchers subsequently improved the synthesis of the heterodimer by adopting the solid-phase peptide synthesis method (Liu et al. 2009b). Further, a spacer (11-amino-3,6,9-trioxaundecanoic acid) was incorporated at the α-amino group of the glutamate to increase the yield of ^{18}F-labeling, as well as to improve the pharmacokinetics. Both goals were indeed achieved in this study with the PC-3 tumor model. It was also suggested that this dual-receptor targeting strategy may provide a general method for developing peptide-based imaging and therapeutic agents with improved in vivo characteristics. The explanation for the superior performance of the heterodimer over the analogous monomers was that if one ligand dissociates from its receptor, the other ligand is in close proximity and can bind to the other receptor closeby. Such phenomenon is similar to the polyvalency effect observed for oligomeric peptides over the analogous monomers (Mammen et al. 1998). However, the key question of whether such heterodimerization is more advantageous than homodimerization remains unanswered. A direct comparison of the radiolabeled BBN-RGD and analogous dimeric BBN, as well as dimeric RGD peptides, will be needed in future studies to elucidate this aspect.

^{68}Ga-labeled BBN analogs

The recent introduction of ^{68}Ga into clinical practice ushers in a new era of PET tracer development which is not dependent on an on-site cyclotron (Al-Nahhas et al. 2007). ^{68}Ga can be generated from a ^{68}Ge/^{68}Ga generator and allows possible kit formulation for routine clinical use. More importantly, it has a high positron yield (89%) which is desirable for PET imaging. In one report, a ^{68}Ga-labeled BBN derivative was investigated (Zhang et al. 2007). This tracer had high affinity and specificity for GRPR, resulting in high uptake in the tumor and the pancreas. Low uptake of the tracer in the liver and fast urinary clearance, which is unfavorable for imaging primary PCa, however, gave high T/N ratio. The major disadvantage of this tracer is the relatively high intestinal activity, which severely limits its potential clinical applications. Recently, ^{68}Ga was also used to label the abovementioned dual-receptor targeting heterodimer, BBN-RGD, with NOTA as the chelator (Liu et al. 2009a). The dual-receptor targeting capability of ^{68}Ga-NOTA-BBN-RGD was again demonstrated in the PC-3 tumor model. One undesirable property of ^{68}Ga-based tracers is the high energy of the positron, which has longer positron range than other PET isotopes (e.g. ^{18}F and ^{64}Cu) and compromises the spatial resolution of the PET image (Levin and Hoffman 1999; Phelps et al. 1975).

Radiolabeled BBN peptide and its derivatives have provided much insight into the biological nature of PCa over the last decade. Among the BBN-based tracers described above, ^{18}F-labeled BBN derivatives perhaps have the brightest future in the clinic. However, they are more suitable for imaging metastatic PCa rather than primary PCa since renal clearance of these tracers is a major concern. Besides these widely used BBN derivatives, other peptides may also be useful for PCa imaging. Recently, ^{11}C-glycylsarcosine was reported to be capable of targeting the H$^+$/peptide transporter (Mitsuoka et al. 2008), which is functionally expressed in many cancer cell lines including PCa but not in inflammatory tissues. This tracer may be advantageous over ^{18}F-FDG in certain scenarios of cancer imaging since ^{18}F-FDG uptake in the inflammatory tissue has long been a major limitation that hampers its sensitivity and specificity (Zhuang et al. 2005).

Phage display and other high throughput screening technology may give rise to novel PCa specific peptides that can be radiolabeled for PET imaging of PCa in the future (Brissette and Goldstein 2007; Landon et al. 2004; Uttamchandani and Yao 2008). For example, one such peptide (DUP-1) has been identified with phage display and tested for PCa imaging (Zitzmann et al. 2005). To generate PET tracers with better metabolic stability, the "Achilles' heel" of

most naturally occurring peptides, peptoids (N-substituted glycines) deserve much research effort in the future. Peptoids are closely related to natural peptides but differ chemically in that the side chains are appended to the nitrogen atoms along the molecule's backbone, which makes them highly resistant to enzyme degradation in vivo (Udugamasooriya et al. 2008). Lastly, antibody and antibody fragments are also attractive alternatives for PET imaging of PCa because of their high affinity and specificity to the corresponding antigen(s).

Radiolabeled antibodies for PET imaging of PCa

The most extensively studied antigen in PCa for antibody-based imaging is the PSMA, a 120-kDa transmembrane type II glycoprotein (Sweat et al. 1998). To date, the physiological function of PSMA remains unclear although it is generally believed that it may be involved in the metastatic process. Studies have shown that PSMA expression in normal prostatic tissues is less than that in the malignant prostate and its metastases (Carter et al. 1996). Radiolabeled antibodies against PSMA have been used in the clinic for the diagnosis of PCa and an ^{111}In-labeled monoclonal antibody, capromab-pendetide, has been extensively evaluated for SPECT imaging applications (Sodee et al. 2005). It is primarily used for the detection of advanced, recurrent PCa and lymph node metastases. However, the clinical utility of capromab-pendetide is highly debated due to its low sensitivity (~ 70%) caused by slow tumor uptake and poor clearance rate from the blood (Brassell et al. 2005). Another major disadvantage of capromabpendetide is that it recognizes an intramembrane epitope of the PSMA, which severely limits its utility in detecting viable cells within the PCa tissue (Barren et al. 1997).

Another antibody which recognizes the extracellular domain of the PSMA has been designed and investigated for localization and staging of PCa (Nargund et al. 2005). However, to the best of our knowledge, no PET isotope-labeled anti-PSMA antibody has been reported for PCa imaging to date. In fact, very few reports of radioimmunoPET of PCa exist in the literature. All these radioimmunoPET studies were carried out in the pre-clinical stage with mouse models, most of which targeted antigens that are not specific for PCa. For example, a chimeric monoclonal antibody that binds phosphatidylserine was labeled with [74]As (half-life: 17.5 days) for PET imaging of PCa in a rat model (Jennewein et al. 2008). Antibodies against integrin $\alpha_v\beta_3$ or EphA2, respectively, have also been labeled with ^{64}Cu and tested in a number of tumor models including PCa (Cai et al. 2007b; Cai et al. 2006). The two studies related to another antigen that is not PCa specific, the epidermal growth factor receptor (EGFR), deserve some attention.

EGFR is a 170-kDa cell surface protein over-expressed in many epithelial cancers including PCa (Cai et al. 2008b; Niu et al. 2008b). Dysregulation of EGFR is associated with several key features of cancer, such as autonomous cell growth, inhibition of apoptosis, angiogenic potential, invasion and metastases (Normanno et al. 2006; Schlessinger 2000). We reported the first quantitative PET imaging of EGFR expression in xenograft-bearing mice using ^{64}Cu-labeled cetuximab, a chimeric anti-EGFR monoclonal antibody (Cai et al. 2007a). Using seven xenograft tumor models, the tumor uptake of ^{64}Cu-DOTA-cetuximab measured by PET was correlated with the EGFR expression level quantified by Western blotting (Fig. 7). A good linear correlation ($R^2 = 0.80$) was observed between the ^{64}Cu-DOTA-cetuximab uptake and the EGFR expression level at 48 hours post-injection, when the tumor uptake reached a plateau. This study laid the foundation for quantitative, non-invasive monitoring of the therapeutic effect of certain molecular therapies which can modulate the EGFR expression level.

In the follow-up study, the EGFR response to an Hsp90 inhibitor, 17-AAG (17-allyamino-17-demethoxygeldanamycin), was non-invasively evaluated with ^{64}Cu-DOTA-cetuximab in the PC-3 tumor model (Niu et al. 2008a). The activity of Hsp90 promotes the attainment and maintenance of proper conformation of its clients, including EGFR and androgen receptor

which are important for mediating PCa progression (Lattouf et al. 2006; Solit et al. 2003). Nude mice bearing PC-3 tumors were injected intraperitoneally with 17-AAG and then imaged with small-animal PET after intravenous injection of ^{64}Cu-DOTA-cetuximab. It was found that ^{64}Cu-DOTA-cetuximab had prominent tumor activity accumulation in untreated tumors (14.6 ± 2.6 %ID/g) but significantly lower uptake in 17-AAG-treated tumors (8.9 ± 1.6 %ID/g) at 24 hours post-injection. Successful monitoring of the early response to anti-Hsp90 therapy can be invaluable for accurately assessing the therapeutic response of EGFR-positive PCa patients in the clinic.

Besides the abovementioned reports which focused on the "universal" targets of cancer, the ^{124}I-labeled 1G8 monoclonal antibody against the PSCA is more PCa specific (Olafsen et al. 2007). PSCA is a cysteine-rich, glycosylphosphatidylinositol-anchored surface glycoprotein which is over-expressed in PCa (including the hormone refractory disease), highly suitable for antibody- or antibody fragment-mediated imaging and/or therapeutical applications (Gu et al. 2000; Reiter et al. 1998). In this study, the murine version of 1G8 was labeled with ^{111}In for SPECT imaging and the humanized version was labeled with ^{124}I for PET imaging of PCa, respectively (Olafsen et al. 2007). Specific tumor targeting of ^{124}I-hu1G8 to PC-3-PSCA xenografts was observed, which supported further development of hu1G8 for targeted imaging and therapy of PCa.

Radiolabeled antibody fragments for PET imaging of PCa

Despite the fact that intact antibodies have high affinity and specificity for tumor-associated antigens, they suffer significantly from long circulation half-lives. Due to the high background signal in the blood pool, PET scans of intact antibody-based tracers are typically carried out at 1 day or several days after injection. To solve this problem, engineered antibody fragments with appropriate pharmacokinetic properties have been developed. These fragments, in particular diabodies and minibodies, can also be bivalent and retain the antigen-binding affinity but with much faster clearance rate from the blood. Diabodies are the dimeric forms of scFv with molecular weight of about 55 kDa, while minibodies are scFv-C_H3 dimer with molecular weight of about 80 kDa (Fig. 8) (Cai et al. 2007c;Filpula 2007;Wu and Senter 2005). Both types of antibody fragment have been demonstrated to possess improved pharmacokinetics over intact antibodies and exhibit high T/N ratios at early time points, which are highly desirable for PET imaging applications.

The available literature of both minibody- and diabody-based PET imaging of PCa targeted the same antigen: the PSCA (Leyton et al. 2008a; Leyton et al. 2008b). Previous preclinical investigations have confirmed the usefulness of 1G8 and hu1G8, the murine and humanized monoclonal antibody against PSCA respectively, for localizing specifically to PSCA-positive tumors (Olafsen et al. 2007). A hu1G8-based minibody was engineered for PET imaging of PCa in xenograft models upon ^{124}I-labeling (Leyton et al. 2008a). Rapid clearance from the blood and non-targeted tissues was observed and both androgen-dependent and androgen-independent tumors were clearly delineated as early as 4 hours post-injection, with further improved image contrast at 21 hours post-injection (Fig. 8a).

PET imaging results with the diabody, engineered from the same parent antibody, were also encouraging (Leyton et al. 2008b). With nanomolar affinity to the antigen (i.e. PSCA), the diabodies were radioiodinated with ^{124}I and evaluated by serial small-animal PET imaging in mice bearing human PCa xenografts. Localization of the tracer in the tumor was seen at 4 hours post-injection, whereas at 20 hours most of the radioactivity had cleared from the tumor (Fig. 8b). Such phenomenon is likely due to the internalization and degradation of the radiolabeled diabody, since free ^{124}I can diffuse virtually freely through the cell membrane and is thus cleared rapidly.

The advantages and disadvantages of PCa imaging and therapeutic agents based on intact antibodies and antibody fragments deserve further investigation. For primary PCa, the low/no renal clearance of intact antibodies (the molecular weight of 150 kDa is well above the renal clearance cut-off, typically 60 kDa) is a plus for imaging applications, provided that the optimal antigen/antibody pair can be identified. Further, the high absolute tumor uptake of intact antibody-based agents also makes them more suitable for PCa-targeted therapy (e.g. radioimmunotherapy and drug delivery). Engineered antibody fragments typically undergo partial renal clearance, which can dampen the enthusiasm for their applications in primary PCa imaging. For PET imaging of metastatic PCa, there are different requirements since radioactivity in the bladder is not a concern. Thus, suitably engineered antibody fragments are certainly more appropriate. The possibility of labeling small antibody fragments with the widely available ^{18}F can also allow for broad use of well validated PET tracers in future clinical studies.

Pre-targeting is another strategy worth exploring for improving the T/N ratio for PET imaging of PCa (Sharkey et al. 2005). Typically, a bispecific antibody is used for pre-targeting. A certain waiting period is needed for the first agent to clear from the circulation and reach the tumor site. After that, a second agent is administered which will target and bind to the first agent, thus giving excellent tumor contrast if the system is designed properly. The disadvantage of pretargeting is that it is much more complex than imaging with a single PET tracer thus is more difficult to translate into the clinic.

Conclusion and future perspectives

Since ^{18}F-FDG PET does not meet the clinical need for PCa imaging, a wide variety of PET tracers have been developed over the last decade. These tracers span an enormous size range, including small molecules (a few hundred Da), single amino acids (100–200 Da), peptides (typically 1–2 kDa), antibody fragments (50–100 kDa), and intact antibodies (~150 kDa). Many of these agents have entered clinical trials. Each class of these PET tracers has unique advantages and disadvantages as previously discussed in this review. For small molecule-based PET tracers, ^{18}F-choline and ^{18}F-FDHT seem to be the most promising for PCa imaging. Among the amino acid-based PET tracers, the results from ^{11}C-methionine are the most encouraging. For peptide-based tracers, BBN peptide and its derivatives are the mainstay and the development/validation of new homodimeric/heterodimeric peptide-based PET tracers deserves much further effort. PET imaging of PCa with antibody- or antibody fragment-based tracers are relatively rare, partly due to the lack of suitable antigen-antibody (fragment) pairs.

To generate a clinically useful PET tracer for PCa imaging, many properties need to be considered simultaneously, such as the right PET isotope to be used (e.g. [18]F is more suitable for peptide and amino acid labeling while long-lived isotopes, such as [74]As, are more suitable for antibody labeling), high metabolic stability (e.g. non-naturally occurring peptoids are more desirable than peptides for tracer development), suitable pharmacokinetic properties (e.g. fast blood clearance), low non-specific accumulation in normal tissues (e.g. appropriate hydrophilicity and molecular weight of the tracer), and high tumor uptake (e.g. agonist vs. antagonist; high affinity/specificity to the target). One aspect that is often overlooked is the high radiolabeling yield, the key requirement for broad future use of any PET tracer in the clinic. Continuous optimization of the radiochemistry certainly deserves due effort.

There are two critical needs for PET imaging of PCa, with the first being accurate early detection of primary lesions. When diagnosed early, the 5-year survival rate of PCa is almost 100% (Otto and de Koning 2004). In the 1990s, the discovery of PSA dramatically improved the early detection of PCa and it has become an indispensable marker for diagnosis and follow-up of PCa patients. However, PSA is not cancer specific which results in significant numbers

of false-positive cases (Schroder et al. 2008; Thompson and Ankerst 2007). New markers that better differentiate benign from malignant lesions and indolent from aggressive PCa are needed to decrease the potential over-treatment of PCa patients. Besides identifying novel blood biomarkers, identification of molecular markers which are upregulated during the early stages of malignancy, using the genomic and proteomic approach, is very important for the development of novel PET tracers for early detection of PCa. For patients that have not been diagnosed with PCa, the aim of PET imaging is to distinguish PCa from benign tissue which can either justify a biopsy or estimate the risk that PCa will develop.

Second, accurate PET imaging of PCa bone metastasis will revolutionize PCa patient management. Bone metastases represent the predominant manifestation for most patients and the primary cause of morbidity and mortality in PCa (Logothetis et al. 2008; Pinski and Dorff 2005). For patients with metastatic PCa, the aim of PET imaging is several fold: to determine whether patients can be selected for a particular therapy based on the tumor biology or whether the presence of certain signalling pathways can predict the outcomes; to determine the pre-treatment extent of disease; and to follow post-treatment effects from therapeutic intervention. To date, there is no generally accepted means for such applications. Most peptide-based PET tracers do not show obvious advantage over ^{18}F-FDG in detecting bone metastasis with the exception of ^{11}C-methionine. ^{18}F-FDHT has been reported to localize to tumor sites in a small number of metastatic PCa patients (Larson et al. 2004). The ideal PET tracer(s) for imaging of PCa bone metastasis remain to be developed in the future.

PET imaging alone may not be sufficient for monitoring the therapeutic efficacy of PCa. The combination of ex vivo diagnostics and in vivo PET imaging can markedly impact PCa patient management by providing a synergistic approach that neither strategy alone can offer. Patients can have their tumors biopsied and blood samples drawn for protein profiling by ex vivo methods to predict their response to a given therapy. In addition, they may also be imaged with suitable PET tracers to predict their response. Post-treatment and potentially during treatment, patient response can be evaluated by both blood analysis and molecular imaging to ensure the accurate differentiation of responders from non-responders. Upon further development and optimization/validation, combination of such ex vivo and in vivo approaches will eventually be able to predict which patients will likely respond to a given therapy and monitor their response to personalized PCa management. The combination of molecular (e.g. PET) and anatomical/functional (e.g. CT and MRI) imaging modalities will be a powerful tool. Active involvement of and interactions among academic researchers, clinicians, pharmaceutical industries, and government agencies are needed to enable rapid first-in-human evaluations and subsequent clinical trials of the most promising PET tracers, thereby ushering in a new era of personalized medicine for PCa patients.

Acknowledgments

References

Agrawal S, Patil KP, Dunsmuir WD. Molecular markers in prostate cancer. Part II: potential roles in management. Asian J Androl 2009;11:22–27. [PubMed: 19050689]

Al-Nahhas A, Win Z, Szyszko T, Singh A, Khan S, Rubello D. What can gallium-68 PET add to receptor and molecular imaging? Eur J Nucl Med Mol Imaging 2007;34:1897–1901. [PubMed: 17713764]

Albrecht S, Buchegger F, Soloviev D, Zaidi H, Vees H, Khan HG, Keller A, Bischof Delaloye A, Ratib O, Miralbell R. ^{11}C-acetate PET in the early evaluation of prostate cancer recurrence. Eur J Nucl Med Mol Imaging 2007;34:185–196. [PubMed: 16832632]

Ananias HJ, de Jong IJ, Dierckx RA, van de Wiele C, Helfrich W, Elsinga PH. Nuclear imaging of prostate cancer with gastrin-releasing-peptide-receptor targeted radiopharmaceuticals. Curr Pharm Des 2008;14:3033–3047. [PubMed: 18991717]

Apolo AB, Pandit-Taskar N, Morris MJ. Novel tracers and their development for the imaging of metastatic prostate cancer. J Nucl Med 2008;49:2031–2041. [PubMed: 18997047]

Barren RJ 3rd, Holmes EH, Boynton AL, Misrock SL, Murphy GP. Monoclonal antibody 7E11.C5 staining of viable LNCaP cells. Prostate 1997;30:65–68. [PubMed: 9018338]

Bartholdi MF, Wu JM, Pu H, Troncoso P, Eden PA, Feldman RI. In situ hybridization for gastrin-releasing peptide receptor (GRP receptor) expression in prostatic carcinoma. Int J Cancer 1998;79:82–90. [PubMed: 9495364]

Beheshti M, Vali R, Waldenberger P, Fitz F, Nader M, Loidl W, Broinger G, Stoiber F, Fogelman I, Langsteger W. Detection of bone metastases in patients with prostate cancer by F-18 fluorocholine and F-18 fluoride PET-CT: a comparative study. Eur J Nucl Med Mol Imaging. 2008

Biddlecombe GB, Rogers BE, de Visser M, Parry JJ, de Jong M, Erion JL, Lewis JS. Molecular imaging of gastrin-releasing peptide receptor-positive tumors in mice using ^{64}Cu- and ^{86}Y-DOTA-(Pro^1,Tyr^4)-bombesin(1–14). Bioconjug Chem 2007;18:724–730. [PubMed: 17378600]

Bouchelouche K, Oehr P. Positron emission tomography and positron emission tomography/computerized tomography of urological malignancies: an update review. J Urol 2008;179:34–45. [PubMed: 17997425]

Brassell SA, Rosner IL, McLeod DG. Update on magnetic resonance imaging, ProstaScint, and novel imaging in prostate cancer. Curr Opin Urol 2005;15:163–166. [PubMed: 15815192]

Brissette R, Goldstein NI. The use of phage display peptide libraries for basic and translational research. Methods Mol Biol 2007;383:203–213. [PubMed: 18217687]

Cai W, Chen K, He L, Cao Q, Koong A, Chen X. Quantitative PET of EGFR expression in xenograft-bearing mice using ^{64}Cu-labeled cetuximab, a chimeric anti-EGFR monoclonal antibody. Eur J Nucl Med Mol Imaging 2007a;34:850–858. [PubMed: 17262214]

Cai W, Chen X. Anti-angiogenic cancer therapy based on integrin $\alpha_v\beta_3$ antagonism. Anti-Cancer Agents Med Chem 2006;6:407–428.

Cai W, Ebrahimnejad A, Chen K, Cao Q, Li ZB, Tice DA, Chen X. Quantitative radioimmunoPET imaging of EphA2 in tumor-bearing mice. Eur J Nucl Med Mol Imaging 2007b;34:2024–2036. [PubMed: 17673999]

Cai W, Niu G, Chen X. Imaging of integrins as biomarkers for tumor angiogenesis. Curr Pharm Des 2008a;14:2943–2973. [PubMed: 18991712]

Cai W, Niu G, Chen X. Multimodality imaging of the HER-kinase axis in cancer. Eur J Nucl Med Mol Imaging 2008b;35:186–208. [PubMed: 17846765]

Cai W, Olafsen T, Zhang X, Cao Q, Gambhir SS, Williams LE, Wu AM, Chen X. PET imaging of colorectal cancer in xenograft-bearing mice by use of an ^{18}F-labeled T84.66 anti-carcinoembryonic antigen diabody. J Nucl Med 2007c;48:304–310. [PubMed: 17268029]

Cai W, Wu Y, Chen K, Cao Q, Tice DA, Chen X. In vitro and in vivo characterization of ^{64}Cu-labeled Abegrin, a humanized monoclonal antibody against integrin $\alpha_v\beta_3$. Cancer Res 2006;66:9673–9681. [PubMed: 17018625]

Carter RE, Feldman AR, Coyle JT. Prostate-specific membrane antigen is a hydrolase with substrate and pharmacologic characteristics of a neuropeptidase. Proc Natl Acad Sci USA 1996;93:749–753. [PubMed: 8570628]

Cescato R, Maina T, Nock B, Nikolopoulou A, Charalambidis D, Piccand V, Reubi JC. Bombesin receptor antagonists may be preferable to agonists for tumor targeting. J Nucl Med 2008;49:318–326. [PubMed: 18199616]

Chang SS, Reuter VE, Heston WD, Bander NH, Grauer LS, Gaudin PB. Five different anti-prostate-specific membrane antigen (PSMA) antibodies confirm PSMA expression in tumor-associated neovasculature. Cancer Res 1999;59:3192–3198. [PubMed: 10397265]

Chen X, Park R, Hou Y, Tohme M, Shahinian AH, Bading JR, Conti PS. microPET and autoradiographic imaging of GRP receptor expression with ^{64}Cu-DOTA-[Lys^3]bombesin in human prostate adenocarcinoma xenografts. J Nucl Med 2004;45:1390–1397. [PubMed: 15299066]

Cornelio DB, Roesler R, Schwartsmann G. Gastrin-releasing peptide receptor as a molecular target in experimental anticancer therapy. Ann Oncol 2007;18:1457–1466. [PubMed: 17351255]

Cury FL, Shenouda G, Souhami L, Duclos M, Faria SL, David M, Verhaegen F, Corns R, Falco T. Ultrasound-based image guided radiotherapy for prostate cancer: comparison of cross-modality and intramodality methods for daily localization during external beam radiotherapy. Int J Radiat Oncol Biol Phys 2006;66:1562–1567. [PubMed: 17056194]

de Jong IJ, Pruim J, Elsinga PH, Jongen MM, Mensink HJ, Vaalburg W. Visualisation of bladder cancer using ^{11}C-choline PET: first clinical experience. Eur J Nucl Med Mol Imaging 2002;29:1283–1288. [PubMed: 12271408]

DeGrado TR, Kwee SA, Coel MN, Coleman RE. The impact of urinary excretion of ^{18}F-labeled choline analogs. J Nucl Med 2007;48:1225. [PubMed: 17607041]

Dehdashti F, Picus J, Michalski JM, Dence CS, Siegel BA, Katzenellenbogen JA, Welch MJ. Positron tomographic assessment of androgen receptors in prostatic carcinoma. Eur J Nucl Med Mol Imaging 2005;32:344–350. [PubMed: 15726353]

Effert PJ, Bares R, Handt S, Wolff JM, Bull U, Jakse G. Metabolic imaging of untreated prostate cancer by positron emission tomography with ^{18}F-labeled deoxyglucose. J Urol 1996;155:994–998. [PubMed: 8583625]

Eisenberger MA, Blumenstein BA, Crawford ED, Miller G, McLeod DG, Loehrer PJ, Wilding G, Sears K, Culkin DJ, Thompson IM Jr, Bueschen AJ, Lowe BA. Bilateral orchiectomy with or without flutamide for metastatic prostate cancer. N Engl J Med 1998;339:1036–1042. [PubMed: 9761805]

Emonds KM, Swinnen JV, Mortelmans L, Mottaghy FM. Molecular imaging of prostate cancer. Methods 2009;48:193–199. [PubMed: 19362147]

Eriksson B, Bergstrom M, Lilja A, Ahlstrom H, Langstrom B, Oberg K. Positron emission tomography (PET) in neuroendocrine gastrointestinal tumors. Acta Oncol 1993;32:189–196. [PubMed: 7686763]

Erspamer V, Erpamer GF, Inselvini M. Some pharmacological actions of alytesin and bombesin. J Pharm Pharmacol 1970;22:875–876. [PubMed: 4395815]

Farsad M, Schiavina R, Castellucci P, Nanni C, Corti B, Martorana G, Canini R, Grigioni W, Boschi S, Marengo M, Pettinato C, Salizzoni E, Monetti N, Franchi R, Fanti S. Detection and localization of prostate cancer: correlation of ^{11}C-choline PET/CT with histopathologic step-section analysis. J Nucl Med 2005;46:1642–1649. [PubMed: 16204714]

Farsad M, Schiavina R, Franceschelli A, Sanguedolce F, Castellucci P, Bertaccini A, Brunocilla E, Manferrari F, Concetti S, Garofalo M, Rocca C, Borghesi M, Franchi R, Fanti S, Nanni C, Martorana G. Positron-emission tomography in imaging and staging prostate cancer. Cancer Biomark 2008;4:277–284. [PubMed: 18957716]

Filpula D. Antibody engineering and modification technologies. Biomol Eng 2007;24:201–215. [PubMed: 17466589]

Foss CA, Mease RC, Fan H, Wang Y, Ravert HT, Dannals RF, Olszewski RT, Heston WD, Kozikowski AP, Pomper MG. Radiolabeled small-molecule ligands for prostate-specific membrane antigen: in vivo imaging in experimental models of prostate cancer. Clin Cancer Res 2005;11:4022–4028. [PubMed: 15930336]

Froidevaux S, Eberle AN. Somatostatin analogs and radiopeptides in cancer therapy. Biopolymers 2002;66:161–183. [PubMed: 12385036]

Fuchsjager M, Shukla-Dave A, Akin O, Barentsz J, Hricak H. Prostate cancer imaging. Acta Radiol 2008;49:107–120. [PubMed: 18210320]

Gambhir SS. Molecular imaging of cancer with positron emission tomography. Nat Rev Cancer 2002;2:683–693. [PubMed: 12209157]

Gambhir SS, Czernin J, Schwimmer J, Silverman DH, Coleman RE, Phelps ME. A tabulated summary of the FDG PET literature. J Nucl Med 2001;42:1S–93S. [PubMed: 11483694]

Garrison JC, Rold TL, Sieckman GL, Figueroa SD, Volkert WA, Jurisson SS, Hoffman TJ. In vivo evaluation and small-animal PET/CT of a prostate cancer mouse model using ^{64}Cu bombesin analogs: side-by-side comparison of the CB-TE2A and DOTA chelation systems. J Nucl Med 2007;48:1327–1337. [PubMed: 17631556]

Gasser G, Tjioe L, Graham B, Belousoff MJ, Juran S, Walther M, Kunstler JU, Bergmann R, Stephan H, Spiccia L. Synthesis, copper(II) complexation, ^{64}Cu-labeling, and bioconjugation of a new bis(2-

pyridylmethyl) derivative of 1,4,7-triazacyclononane. Bioconjug Chem 2008;19:719–730. [PubMed: 18254581]

Goodman MM DVJ, Kabalka GW. Microprocessor-controlled open vessel system for the production of no-carrier-added-1-aminocyclobutane-1-carboxylic acid. J Labelled Compds Radiopharm 1994;35:331–333.

Gu Z, Thomas G, Yamashiro J, Shintaku IP, Dorey F, Raitano A, Witte ON, Said JW, Loda M, Reiter RE. Prostate stem cell antigen (PSCA) expression increases with high gleason score, advanced stage and bone metastasis in prostate cancer. Oncogene 2000;19:1288–1296. [PubMed: 10713670]

Gugger M, Reubi JC. Gastrin-releasing peptide receptors in non-neoplastic and neoplastic human breast. Am J Pathol 1999;155:2067–2076. [PubMed: 10595936]

Hara T, Kosaka N, Kishi H. Development of ^{18}F-fluoroethylcholine for cancer imaging with PET: synthesis, biochemistry, and prostate cancer imaging. J Nucl Med 2002;43:187–199. [PubMed: 11850483]

Heinlein CA, Chang C. Androgen receptor in prostate cancer. Endocr Rev 2004;25:276–308. [PubMed: 15082523]

Hinkle GH, Burgers JK, Neal CE, Texter JH, Kahn D, Williams RD, Maguire R, Rogers B, Olsen JO, Badalament RA. Multicenter radioimmunoscintigraphic evaluation of patients with prostate carcinoma using indium-111 capromab pendetide. Cancer 1998;83:739–747. [PubMed: 9708939]

Hricak H, Choyke PL, Eberhardt SC, Leibel SA, Scardino PT. Imaging prostate cancer: a multidisciplinary perspective. Radiology 2007;243:28–53. [PubMed: 17392247]

Hubner KF, Krauss S, Washburn LC, Gibbs WD, Holloway EC. Tumor detection with 1-aminocyclopentane and 1-aminocyclobutane C-11-carboxylic acid using positron emission computerized tomography. Clin Nucl Med 1981;6:249–252. [PubMed: 6971725]

Husarik DB, Miralbell R, Dubs M, John H, Giger OT, Gelet A, Cservenyak T, Hany TF. Evaluation of [^{18}F]-choline PET/CT for staging and restaging of prostate cancer. Eur J Nucl Med Mol Imaging 2008;35:253–263. [PubMed: 17926036]

Jani AB, Fox TH, Whitaker D, Schuster DM. Case study of anti-1-amino-3-F-18 fluorocyclobutane-1-carboxylic acid (anti-[F-18] FACBC) to guide prostate cancer radiotherapy target design. Clin Nucl Med 2009;34:279–284. [PubMed: 19387202]

Jemal A, Siegel R, Ward E, Hao Y, Xu J, Murray T, Thun MJ. Cancer statistics, 2008. CA Cancer J Clin 2008;58:71–96. [PubMed: 18287387]

Jennewein M, Lewis MA, Zhao D, Tsyganov E, Slavine N, He J, Watkins L, Kodibagkar VD, O'Kelly S, Kulkarni P, Antich PP, Hermanne A, Rosch F, Mason RP, Thorpe PE. Vascular imaging of solid tumors in rats with a radioactive arsenic-labeled antibody that binds exposed phosphatidylserine. Clin Cancer Res 2008;14:1377–1385. [PubMed: 18316558]

Kalkner KM, Ginman C, Nilsson S, Bergstrom M, Antoni G, Ahlstrom H, Langstrom B, Westlin JE. Positron emission tomography (PET) with ^{11}C-5-hydroxytryptophan (5-HTP) in patients with metastatic hormone-refractory prostatic adenocarcinoma. Nucl Med Biol 1997;24:319–325. [PubMed: 9257330]

Kurhanewicz J, Bok R, Nelson SJ, Vigneron DB. Current and potential applications of clinical ^{13}C MR spectroscopy. J Nucl Med 2008;49:341–344. [PubMed: 18322118]

Landon LA, Zou J, Deutscher SL. Is phage display technology on target for developing peptide-based cancer drugs? Curr Drug Discov Technol 2004;1:113–132. [PubMed: 16472251]

Larson SM, Morris M, Gunther I, Beattie B, Humm JL, Akhurst TA, Finn RD, Erdi Y, Pentlow K, Dyke J, Squire O, Bornmann W, McCarthy T, Welch M, Scher H. Tumor localization of 16β-^{18}F-fluoro-5α-dihydrotestosterone versus ^{18}F-FDG in patients with progressive, metastatic prostate cancer. J Nucl Med 2004;45:366–373. [PubMed: 15001675]

Larson SM, Schoder H. Advances in positron emission tomography applications for urologic cancers. Curr Opin Urol 2008;18:65–70. [PubMed: 18090493]

Lattouf JB, Srinivasan R, Pinto PA, Linehan WM, Neckers L. Mechanisms of disease: the role of heat-shock protein 90 in genitourinary malignancy. Nat Clin Pract Urol 2006;3:590–601. [PubMed: 17088927]

NIH-PA Author Manuscript

NIH-PA Author Manuscript

NIH-PA Author Manuscript

Laverman P, Boerman OC, Corstens FH, Oyen WJ. Fluorinated amino acids for tumour imaging with positron emission tomography. Eur J Nucl Med Mol Imaging 2002;29:681–690. [PubMed: 11976809]

Lebl M, Hachmann J. High-throughput peptide synthesis. Methods Mol Biol 2005;298:167–194. [PubMed: 16044547]

Levin CS, Hoffman EJ. Calculation of positron range and its effect on the fundamental limit of positron emission tomography system spatial resolution. Phys Med Biol 1999;44:781–799. [PubMed: 10211810]

Lewis JS, Anderson CJ. Radiometal-labeled somatostatin analogs for applications in cancer imaging and therapy. Methods Mol Biol 2007;386:227–240. [PubMed: 18604948]

Leyton JV, Olafsen T, Lepin EJ, Hahm S, Bauer KB, Reiter RE, Wu AM. Humanized radioiodinated minibody for imaging of prostate stem cell antigen-expressing tumors. Clin Cancer Res 2008a; 14:7488–7496. [PubMed: 19010866]

Leyton JV, Olafsen T, Sherman MA, Bauer KB, Aghajanian P, Reiter RE, Wu AM. Engineered humanized diabodies for microPET imaging of prostate stem cell antigen-expressing tumors. Protein Eng Des Sel. 2008b

Li ZB, Wu Z, Chen K, Ryu EK, Chen X. ^{18}F-labeled BBN-RGD heterodimer for prostate cancer imaging. J Nucl Med 2008;49:453–461. [PubMed: 18287274]

Linden RA, Halpern EJ. Advances in transrectal ultrasound imaging of the prostate. Semin Ultrasound CT MR 2007;28:249–257. [PubMed: 17874649]

Liu Z, Niu G, Wang F, Chen X. ^{68}Ga-labeled NOTA-RGD-BBN peptide for dual integrin and GRPR-targeted tumor imaging. Eur J Nucl Med Mol Imaging Epub. 2009a

Liu Z, Yan Y, Chin FT, Wang F, Chen X. Dual integrin and gastrin-releasing peptide receptor targeted tumor imaging using ^{18}F-labeled PEGylated RGD-bombesin heterodimer ^{18}F-FB-PEG3-Glu-RGD-BBN. J Med Chem 2009b;52:425–432. [PubMed: 19113865]

Logothetis CJ, Navone NM, Lin SH. Understanding the biology of bone metastases: key to the effective treatment of prostate cancer. Clin Cancer Res 2008;14:1599–1602. [PubMed: 18347159]

Macapinlac HA, Humm JL, Akhurst T, Osman I, Pentlow K, Shangde C, Yeung HW, Squire O, Finn RD, Scher HI, Larson SM. Differential metabolism and pharmacokinetics of L-[1-^{11}C]-methionine and 2-[^{18}F] fluoro-2-deoxy-D-glucose (FDG) in androgen independent prostate cancer. Clin Positron Imaging 1999;2:173–181. [PubMed: 14516541]

Mammen M, Chio S, Whitesides GM. Polyvalent interactions in biological systems: implications for design and use of multivalent ligands and inhibitors. Angew Chem Int Ed Engl 1998;37:2755–2794.

Manyak MJ. Indium-111 capromab pendetide in the management of recurrent prostate cancer. Expert Rev Anticancer Ther 2008;8:175–181. [PubMed: 18279057]

Markwalder R, Reubi JC. Gastrin-releasing peptide receptors in the human prostate: relation to neoplastic transformation. Cancer Res 1999;59:1152–1159. [PubMed: 10070977]

Mathews D, Oz OK. Positron emission tomography in prostate and renal cell carcinoma. Curr Opin Urol 2002;12:381–385. [PubMed: 12172424]

McConathy J, Goodman MM. Non-natural amino acids for tumor imaging using positron emission tomography and single photon emission computed tomography. Cancer Metastasis Rev 2008;27:555–573. [PubMed: 18648909]

McDonald TJ, Jornvall H, Nilsson G, Vagne M, Ghatei M, Bloom SR, Mutt V. Characterization of a gastrin releasing peptide from porcine non-antral gastric tissue. Biochem Biophys Res Commun 1979;90:227–233. [PubMed: 496973]

Mease RC, Dusich CL, Foss CA, Ravert HT, Dannals RF, Seidel J, Prideaux A, Fox JJ, Sgouros G, Kozikowski AP, Pomper MG. N-[N-[(S)-1,3-Dicarboxypropyl]carbamoyl]-4-[^{18}F]fluorobenzyl-L-cysteine, [^{18}F]DCFBC: a new imaging probe for prostate cancer. Clin Cancer Res 2008;14:3036–3043. [PubMed: 18483369]

Mitsuoka K, Miyoshi S, Kato Y, Murakami Y, Utsumi R, Kubo Y, Noda A, Nakamura Y, Nishimura S, Tsuji A. Cancer detection using a PET tracer, ^{11}C-glycylsarcosine, targeted to H+/peptide transporter. J Nucl Med 2008;49:615–622. [PubMed: 18344442]

Morris MJ, Akhurst T, Larson SM, Ditullio M, Chu E, Siedlecki K, Verbel D, Heller G, Kelly WK, Slovin S, Schwartz L, Scher HI. Fluorodeoxyglucose positron emission tomography as an outcome measure

for castrate metastatic prostate cancer treated with antimicrotubule chemotherapy. Clin Cancer Res 2005;11:3210–3216. [PubMed: 15867215]

Morris MJ, Akhurst T, Osman I, Nunez R, Macapinlac H, Siedlecki K, Verbel D, Schwartz L, Larson SM, Scher HI. Fluorinated deoxyglucose positron emission tomography imaging in progressive metastatic prostate cancer. Urology 2002;59:913–918. [PubMed: 12031380]

Mueller-Lisse UG, Swanson MG, Vigneron DB, Kurhanewicz J. Magnetic resonance spectroscopy in patients with locally confined prostate cancer: association of prostatic citrate and metabolic atrophy with time on hormone deprivation therapy, PSA level, and biopsy Gleason score. Eur Radiol 2007;17:371–378. [PubMed: 16791635]

Nanni C, Castellucci P, Farsad M, Rubello D, Fanti S. ^{11}C/^{18}F-choline PET or ^{11}C/^{18}F-acetate PET in prostate cancer: may a choice be recommended? Eur J Nucl Med Mol Imaging 2007;34:1704–1705. [PubMed: 17619877]

Nargund V, Al Hashmi D, Kumar P, Gordon S, Otitie U, Ellison D, Carroll M, Baithun S, Britton KE. Imaging with radiolabelled monoclonal antibody (MUJ591) to prostate-specific membrane antigen in staging of clinically localized prostatic carcinoma: comparison with clinical, surgical and histological staging. BJU Int 2005;95:1232–1236. [PubMed: 15892807]

Niu G, Cai W, Chen K, Chen X. Non-invasive PET imaging of EGFR degradation induced by a heat shock protein 90 inhibitor. Mol Imaging Biol 2008a;10:99–106. [PubMed: 18157579]

Niu G, Cai W, Chen X. Molecular imaging of human epidermal growth factor receptor 2 (HER-2) expression. Front Biosci 2008b;13:790–805. [PubMed: 17981588]

Norberg M, Egevad L, Holmberg L, Sparen P, Norlen BJ, Busch C. The sextant protocol for ultrasound-guided core biopsies of the prostate underestimates the presence of cancer. Urology 1997;50:562–566. [PubMed: 9338732]

Normanno N, De Luca A, Bianco C, Strizzi L, Mancino M, Maiello MR, Carotenuto A, De Feo G, Caponigro F, Salomon DS. Epidermal growth factor receptor (EGFR) signaling in cancer. Gene 2006;366:2–16. [PubMed: 16377102]

Nunez R, Macapinlac HA, Yeung HW, Akhurst T, Cai S, Osman I, Gonen M, Riedel E, Scher HI, Larson SM. Combined ^{18}F-FDG and ^{11}C-methionine PET scans in patients with newly progressive metastatic prostate cancer. J Nucl Med 2002;43:46–55. [PubMed: 11801702]

Nye JA, Schuster DM, Yu W, Camp VM, Goodman MM, Votaw JR. Biodistribution and radiation dosimetry of the synthetic nonmetabolized amino acid analogue anti-^{18}F-FACBC in humans. J Nucl Med 2007;48:1017–1020. [PubMed: 17504867]

Oka S, Hattori R, Kurosaki F, Toyama M, Williams LA, Yu W, Votaw JR, Yoshida Y, Goodman MM, Ito O. A preliminary study of anti-1-amino-3-^{18}F-fluorocyclobutyl-1-carboxylic acid for the detection of prostate cancer. J Nucl Med 2007;48:46–55. [PubMed: 17204698]

Okarvi SM. Recent progress in fluorine-18 labelled peptide radiopharmaceuticals. Eur J Nucl Med 2001;28:929–938. [PubMed: 11504093]

Olafsen T, Gu Z, Sherman MA, Leyton JV, Witkosky ME, Shively JE, Raubitschek AA, Morrison SL, Wu AM, Reiter RE. Targeting, imaging, and therapy using a humanized antiprostate stem cell antigen (PSCA) antibody. J Immunother 2007;30:396–405. [PubMed: 17457214]

Otto SJ, de Koning HJ. Update on screening and early detection of prostate cancer. Curr Opin Urol 2004;14:151–156. [PubMed: 15069305]

Oyama N, Ponde DE, Dence C, Kim J, Tai YC, Welch MJ. Monitoring of therapy in androgen-dependent prostate tumor model by measuring tumor proliferation. J Nucl Med 2004;45:519–525. [PubMed: 15001697]

Parry JJ, Kelly TS, Andrews R, Rogers BE. In vitro and in vivo evaluation of ^{64}Cu-labeled DOTA-linker-bombesin(7–14) analogues containing different amino acid linker moieties. Bioconjug Chem 2007;18:1110–1117. [PubMed: 17503761]

Pauwels EK, Ribeiro MJ, Stoot JH, McCready VR, Bourguignon M, Maziere B. FDG accumulation and tumor biology. Nucl Med Biol 1998;25:317–322. [PubMed: 9639291]

Phelps ME. PET: the merging of biology and imaging into molecular imaging. J Nucl Med 2000;41:661–681. [PubMed: 10768568]

Phelps ME, Hoffman EJ, Huang SC, Ter-Pogossian MM. Effect of positron range on spatial resolution. J Nucl Med 1975;16:649–652. [PubMed: 1151485]

Pinski J, Dorff TB. Prostate cancer metastases to bone: pathophysiology, pain management, and the promise of targeted therapy. Eur J Cancer 2005;41:932–940. [PubMed: 15808959]

Plathow C, Weber WA. Tumor cell metabolism imaging. J Nucl Med 2008;49:43S–63S. [PubMed: 18523065]

Ponde DE, Dence CS, Oyama N, Kim J, Tai YC, Laforest R, Siegel BA, Welch MJ. ^{18}F-fluoroacetate: a potential acetate analog for prostate tumor imaging--in vivo evaluation of ^{18}F-fluoroacetate versus ^{11}C-acetate. J Nucl Med 2007;48:420–428. [PubMed: 17332620]

Prasanphanich AF, Nanda PK, Rold TL, Ma L, Lewis MR, Garrison JC, Hoffman TJ, Sieckman GL, Figueroa SD, Smith CJ. [^{64}Cu-NOTA-8-Aoc-BBN(7–14)NH$_2$] targeting vector for positron-emission tomography imaging of gastrin-releasing peptide receptor-expressing tissues. Proc Natl Acad Sci USA 2007;104:12462–12467. [PubMed: 17626788]

Price JM, Davidson AJ. Computed tomography in the evaluation of the suspected carcinomatous prostate. Urol Radiol 1979;1:39–42. [PubMed: 95425]

Reader JC. Automation in medicinal chemistry. Curr Top Med Chem 2004;4:671–686. [PubMed: 15032681]

Reiter RE, Gu Z, Watabe T, Thomas G, Szigeti K, Davis E, Wahl M, Nisitani S, Yamashiro J, Le Beau MM, Loda M, Witte ON. Prostate stem cell antigen: a cell surface marker overexpressed in prostate cancer. Proc Natl Acad Sci USA 1998;95:1735–1740. [PubMed: 9465086]

Reubi JC. Targeting CCK receptors in human cancers. Curr Top Med Chem 2007;7:1239–1242. [PubMed: 17584145]

Reubi JC, Maecke HR. Peptide-based probes for cancer imaging. J Nucl Med 2008;49:1735–1738. [PubMed: 18927341]

Rogers BE, Anderson CJ, Connett JM, Guo LW, Edwards WB, Sherman EL, Zinn KR, Welch MJ. Comparison of four bifunctional chelates for radiolabeling monoclonal antibodies with copper radioisotopes: biodistribution and metabolism. Bioconjug Chem 1996;7:511–522. [PubMed: 8853465]

Rogers BE, Bigott HM, McCarthy DW, Della Manna D, Kim J, Sharp TL, Welch MJ. MicroPET imaging of a gastrin-releasing peptide receptor-positive tumor in a mouse model of human prostate cancer using a ^{64}Cu-labeled bombesin analogue. Bioconjug Chem 2003;14:756–763. [PubMed: 12862428]

Rorvik J, Haukaas S. Magnetic resonance imaging of the prostate. Curr Opin Urol 2001;11:181–188. [PubMed: 11224749]

Schlessinger J. Cell signaling by receptor tyrosine kinases. Cell 2000;103:211–225. [PubMed: 11057895]

Schroder FH, Carter HB, Wolters T, van den Bergh RC, Gosselaar C, Bangma CH, Roobol MJ. Early detection of prostate cancer in 2007. Part 1: PSA and PSA kinetics. Eur Urol 2008;53:468–477. [PubMed: 17997011]

Schuster DM, Votaw JR, Nieh PT, Yu W, Nye JA, Master V, Bowman FD, Issa MM, Goodman MM. Initial experience with the radiotracer anti-1-amino-3-^{18}F-fluorocyclobutane-1-carboxylic acid with PET/CT in prostate carcinoma. J Nucl Med 2007;48:56–63. [PubMed: 17204699]

Seltzer MA, Barbaric Z, Belldegrun A, Naitoh J, Dorey F, Phelps ME, Gambhir SS, Hoh CK. Comparison of helical computerized tomography, positron emission tomography and monoclonal antibody scans for evaluation of lymph node metastases in patients with prostate specific antigen relapse after treatment for localized prostate cancer. J Urol 1999;162:1322–1328. [PubMed: 10492189]

Seo Y, Franc BL, Hawkins RA, Wong KH, Hasegawa BH. Progress in SPECT/CT imaging of prostate cancer. Technol Cancer Res Treat 2006;5:329–336. [PubMed: 16866563]

Sharkey RM, Cardillo TM, Rossi EA, Chang CH, Karacay H, McBride WJ, Hansen HJ, Horak ID, Goldenberg DM. Signal amplification in molecular imaging by pretargeting a multivalent, bispecific antibody. Nat Med 2005;11:1250–1255. [PubMed: 16258537]

Shoup TM, Olson J, Hoffman JM, Votaw J, Eshima D, Eshima L, Camp VM, Stabin M, Votaw D, Goodman MM. Synthesis and evaluation of [^{18}F]1-amino-3-fluorocyclobutane-1-carboxylic acid to image brain tumors. J Nucl Med 1999;40:331–338. [PubMed: 10025843]

Silver DA, Pellicer I, Fair WR, Heston WD, Cordon-Cardo C. Prostate-specific membrane antigen expression in normal and malignant human tissues. Clin Cancer Res 1997;3:81–85. [PubMed: 9815541]

Sodee DB, Nelson AD, Faulhaber PF, Maclennan GT, Resnick MI, Bakale G. Update on fused capromab pendetide imaging of prostate cancer. Clin Prostate Cancer 2005;3:230–238. [PubMed: 15882479]

Solit DB, Scher HI, Rosen N. Hsp90 as a therapeutic target in prostate cancer. Semin Oncol 2003;30:709–716. [PubMed: 14571418]

Squillaci E, Manenti G, Mancino S, Carlani M, Di Roma M, Colangelo V, Simonetti G. MR spectroscopy of prostate cancer. Initial clinical experience. J Exp Clin Cancer Res 2005;24:523–530. [PubMed: 16471314]

Sutinen E, Jyrkkio S, Gronroos T, Haaparanta M, Lehikoinen P, Nagren K. Biodistribution of [^{11}C] methylaminoisobutyric acid, a tracer for PET studies on system A amino acid transport in vivo. Eur J Nucl Med 2001;28:847–854. [PubMed: 11504081]

Sweat SD, Pacelli A, Murphy GP, Bostwick DG. Prostate-specific membrane antigen expression is greatest in prostate adenocarcinoma and lymph node metastases. Urology 1998;52:637–640. [PubMed: 9763084]

Texter JH Jr, Neal CE. The role of monoclonal antibody in the management of prostate adenocarcinoma. J Urol 1998;160:2393–2395. [PubMed: 9817390]

Thompson IM, Ankerst DP. Prostate-specific antigen in the early detection of prostate cancer. CMAJ 2007;176:1853–1858. [PubMed: 17576986]

Tolvanen T, Nagren K, Yu M, Sutinen E, Havu-Auren K, Jyrkkio S, Asola M, Kotoneva E, Nuutila P, Minn H. Human radiation dosimetry of [^{11}C]MeAIB, a new tracer for imaging of system A amino acid transport. Eur J Nucl Med Mol Imaging 2006;33:1178–1184. [PubMed: 16721566]

Toth G, Lengyel Z, Balkay L, Salah MA, Tron L, Toth C. Detection of prostate cancer with ^{11}C-methionine positron emission tomography. J Urol 2005;173:66–69. discussion 69. [PubMed: 15592030]

Udugamasooriya DG, Dineen SP, Brekken RA, Kodadek T. A peptoid "antibody surrogate" that antagonizes VEGF receptor 2 activity. J Am Chem Soc 2008;130:5744–5752. [PubMed: 18386897]

Uttamchandani M, Yao SQ. Peptide microarrays: next generation biochips for detection, diagnostics and high-throughput screening. Curr Pharm Des 2008;14:2428–2438. [PubMed: 18781992]

Vavere AL, Kridel SJ, Wheeler FB, Lewis JS. 1-^{11}C-acetate as a PET radiopharmaceutical for imaging fatty acid synthase expression in prostate cancer. J Nucl Med 2008;49:327–334. [PubMed: 18199615]

Vavere AL, Lewis JS. Examining the relationship between Cu-ATSM hypoxia selectivity and fatty acid synthase expression in human prostate cancer cell lines. Nucl Med Biol 2008;35:273–279. [PubMed: 18355682]

Weiner RE, Thakur ML. Radiolabeled peptides in oncology: role in diagnosis and treatment. BioDrugs 2005;19:145–163. [PubMed: 15984900]

Wu AM, Senter PD. Arming antibodies: prospects and challenges for immunoconjugates. Nat Biotechnol 2005;23:1137–1146. [PubMed: 16151407]

Yang YS, Zhang X, Xiong Z, Chen X. Comparative in vitro and in vivo evaluation of two ^{64}Cu-labeled bombesin analogs in a mouse model of human prostate adenocarcinoma. Nucl Med Biol 2006;33:371–380. [PubMed: 16631086]

Zanzonico PB, Finn R, Pentlow KS, Erdi Y, Beattie B, Akhurst T, Squire O, Morris M, Scher H, McCarthy T, Welch M, Larson SM, Humm JL. PET-based radiation dosimetry in man of ^{18}F-fluorodihydrotestosterone, a new radiotracer for imaging prostate cancer. J Nucl Med 2004;45:1966–1971. [PubMed: 15534070]

Zhang H, Schuhmacher J, Waser B, Wild D, Eisenhut M, Reubi JC, Maecke HR. DOTA-PESIN, a DOTA-conjugated bombesin derivative designed for the imaging and targeted radionuclide treatment of bombesin receptor-positive tumours. Eur J Nucl Med Mol Imaging 2007;34:1198–1208. [PubMed: 17262215]

Zhang X, Cai W, Cao F, Schreibmann E, Wu Y, Wu JC, Xing L, Chen X. ^{18}F-labeled bombesin analogs for targeting GRP receptor-expressing prostate cancer. J Nucl Med 2006a;47:492–501. [PubMed: 16513619]

Zhang X, Xiong Z, Wu Y, Cai W, Tseng JR, Gambhir SS, Chen X. Quantitative PET imaging of tumor integrin $\alpha_v\beta_3$ expression with ^{18}F-FRGD2. J Nucl Med 2006b;47:113–121. [PubMed: 16391195]

Zhuang H, Yu JQ, Alavi A. Applications of fluorodeoxyglucose-PET imaging in the detection of infection and inflammation and other benign disorders. Radiol Clin North Am 2005;43:121–134. [PubMed: 15693652]

Zitzmann S, Mier W, Schad A, Kinscherf R, Askoxylakis V, Kramer S, Altmann A, Eisenhut M, Haberkorn U. A new prostate carcinoma binding peptide (DUP-1) for tumor imaging and therapy. Clin Cancer Res 2005;11:139–146. [PubMed: 15671538]

Zwanziger D, Khan IU, Neundorf I, Sieger S, Lehmann L, Friebe M, Dinkelborg L, Beck-Sickinger AG. Novel chemically modified analogues of neuropeptide Y for tumor targeting. Bioconjug Chem 2008;19:1430–1438. [PubMed: 18572959]
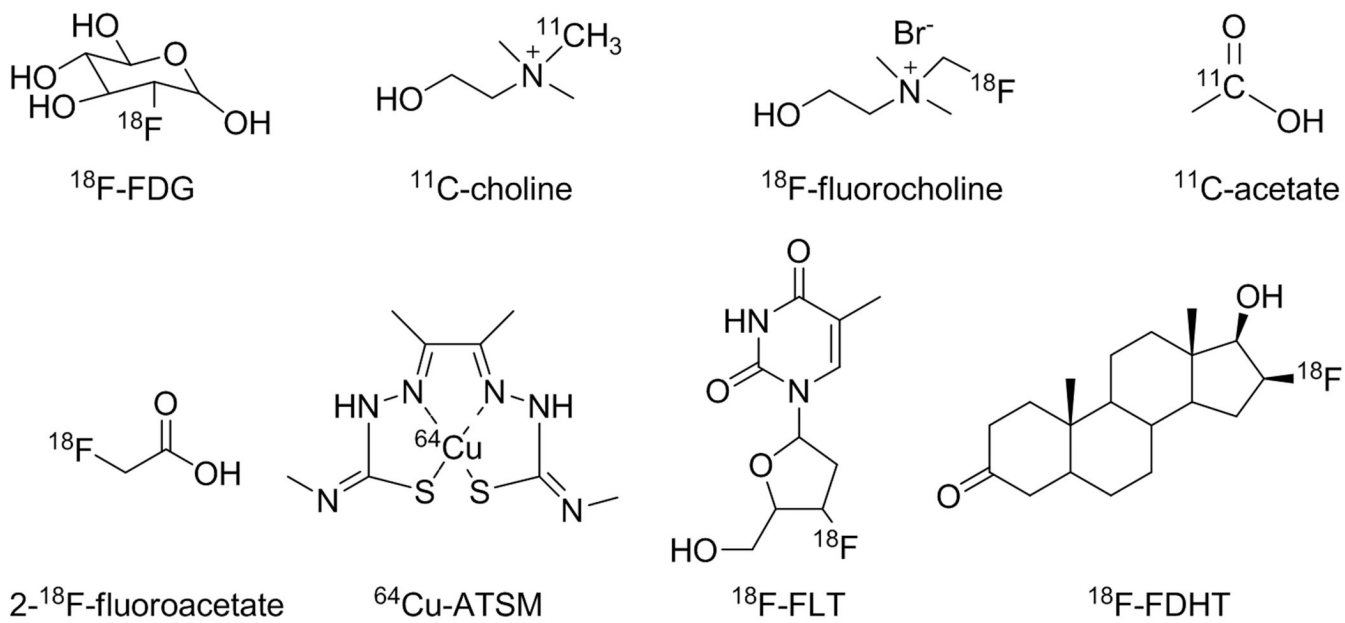
Fig. 1.
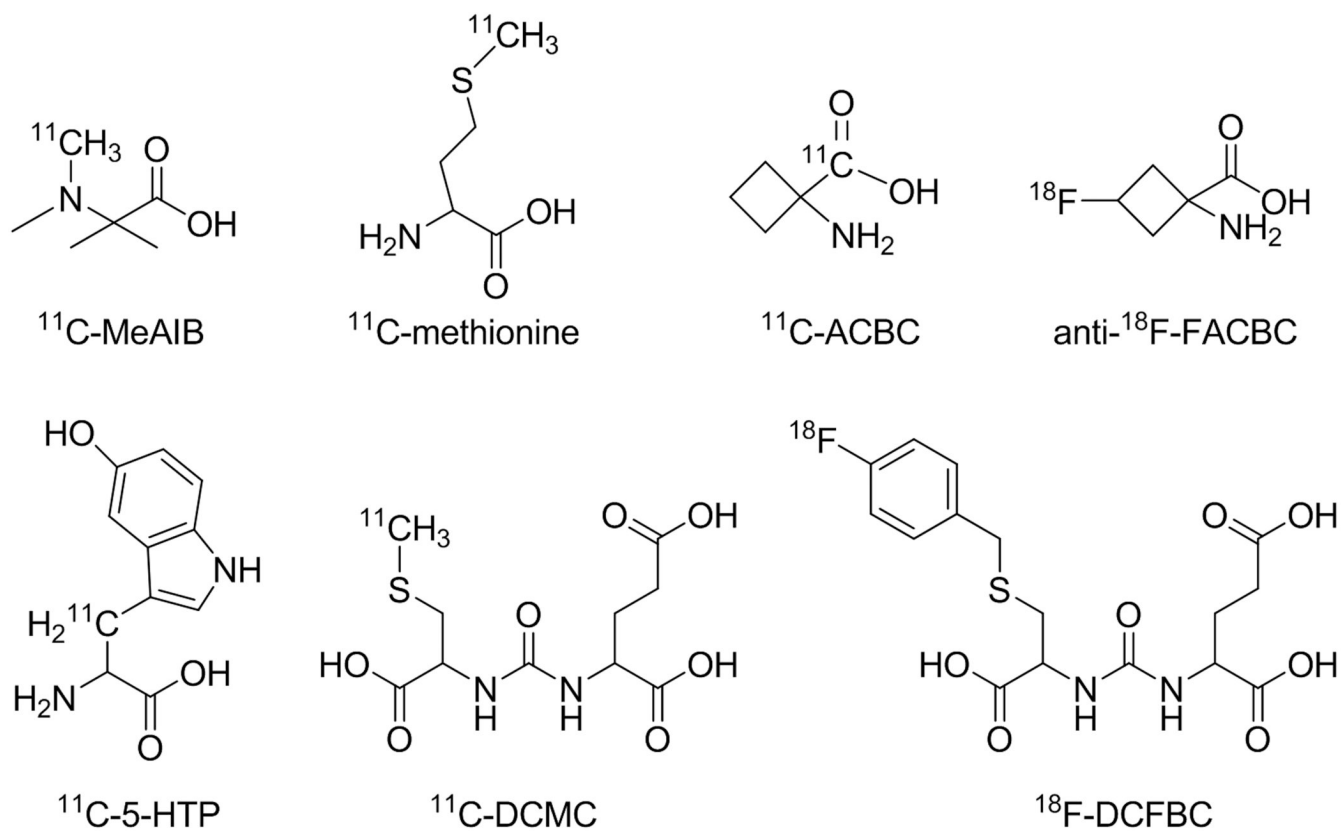Representative small molecule-based PET tracers for PCa imaging

Fig. 2.
Representative radiolabeled amino acid derivatives for PET imaging of PCa
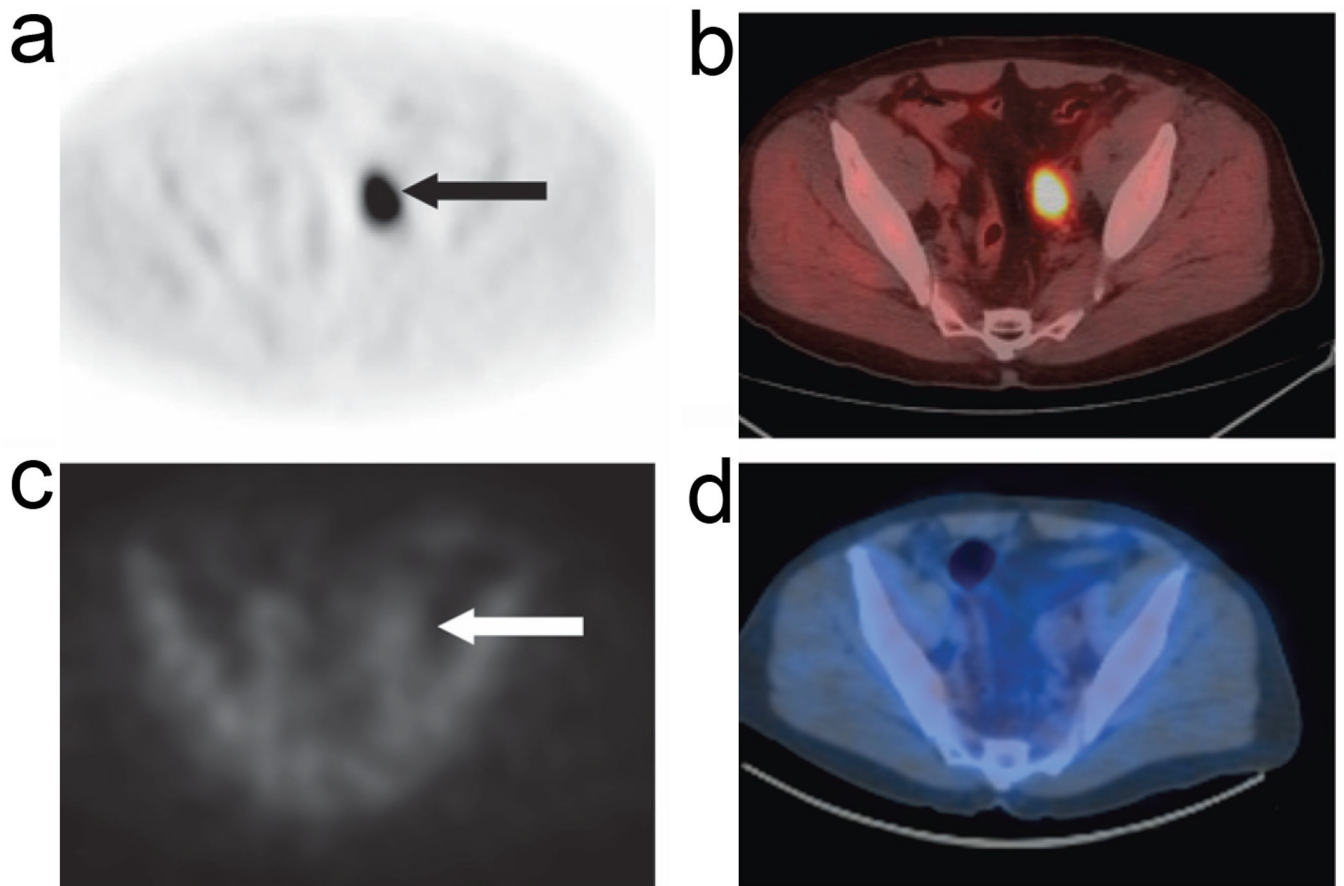
Fig. 3.
PET imaging of PCa with ^{18}F-FACBC. Axial PET (**a**) and PET/CT (**b**) images of a PCa patient, after injection with ^{18}F-FACBC, revealed intense activity in the left external iliac node (black arrow in **a**). SPECT/CT with ^{111}In-capromab-pendetide (**c** & **d**) exhibited no significant radioactivity in this region (white arrow in **c**). Adapted from (Schuster et al. 2007)
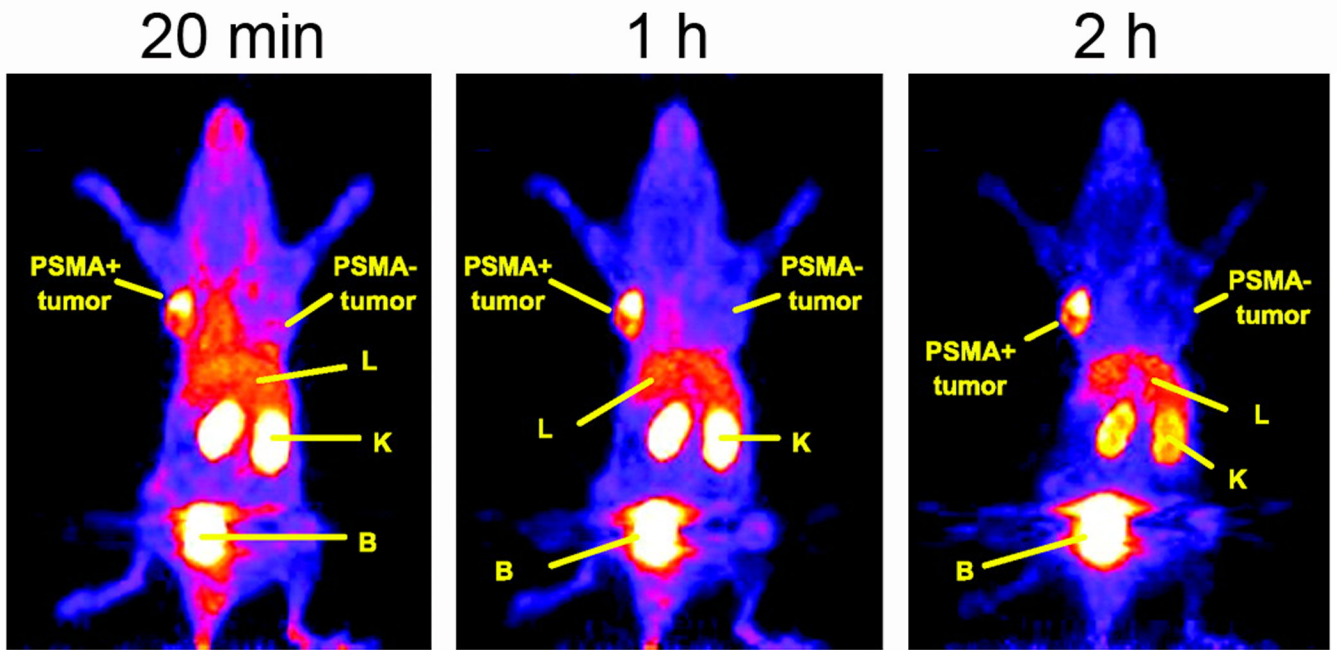
Fig. 4.
Serial PET images of mice bearing both PSMA-positive and PSMA-negative tumors after intravenous injection of ^{18}F-DCFBC. L: Liver; K: kidney; B: bladder. Adapted from (Mease et al. 2008)
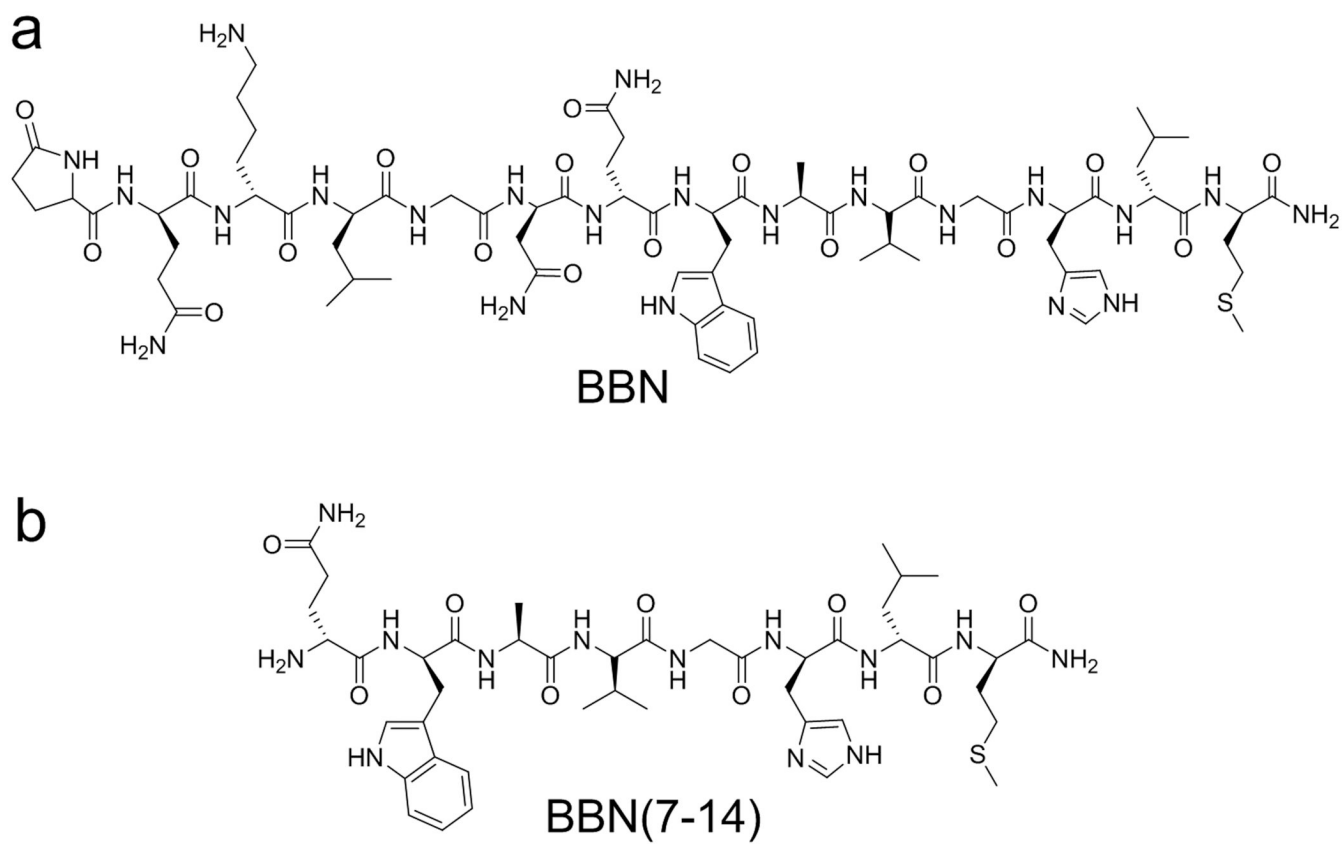
Fig. 5.
Chemical structures of BBN (**a**) and its truncated derivative, BBN(7–14) (**b**)
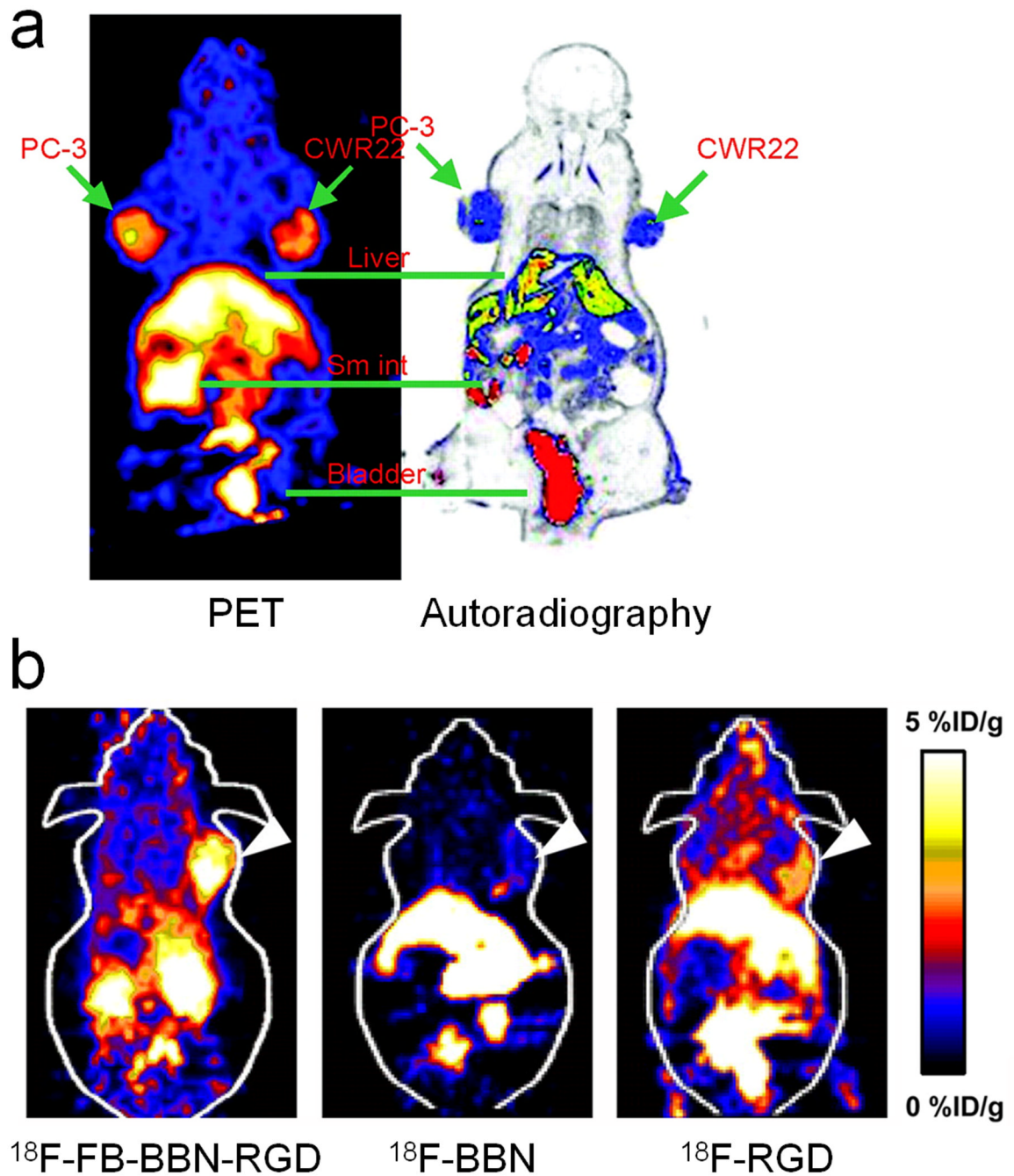
Fig. 6.
PET imaging of GRPR expression in PCa models. (**a**) Left: A coronal PET image of a PC-3 and CWR22 tumor-bearing mouse at 1 hour post-injection of ^{64}Cu-DOTA-[Lys^3]BBN. Right: Digital autoradiograph of the mouse tissue section containing the tumors. (**b**) Decay-corrected whole-body coronal PET images of PC-3 tumor-bearing mice at 30 minutes post-injection of ^{18}F-FB-BBN-RGD, ^{18}F-BBN, or ^{18}F-RGD. Tumors are indicated by arrowheads. Adapted from (Chen et al. 2004; Li et al. 2008)
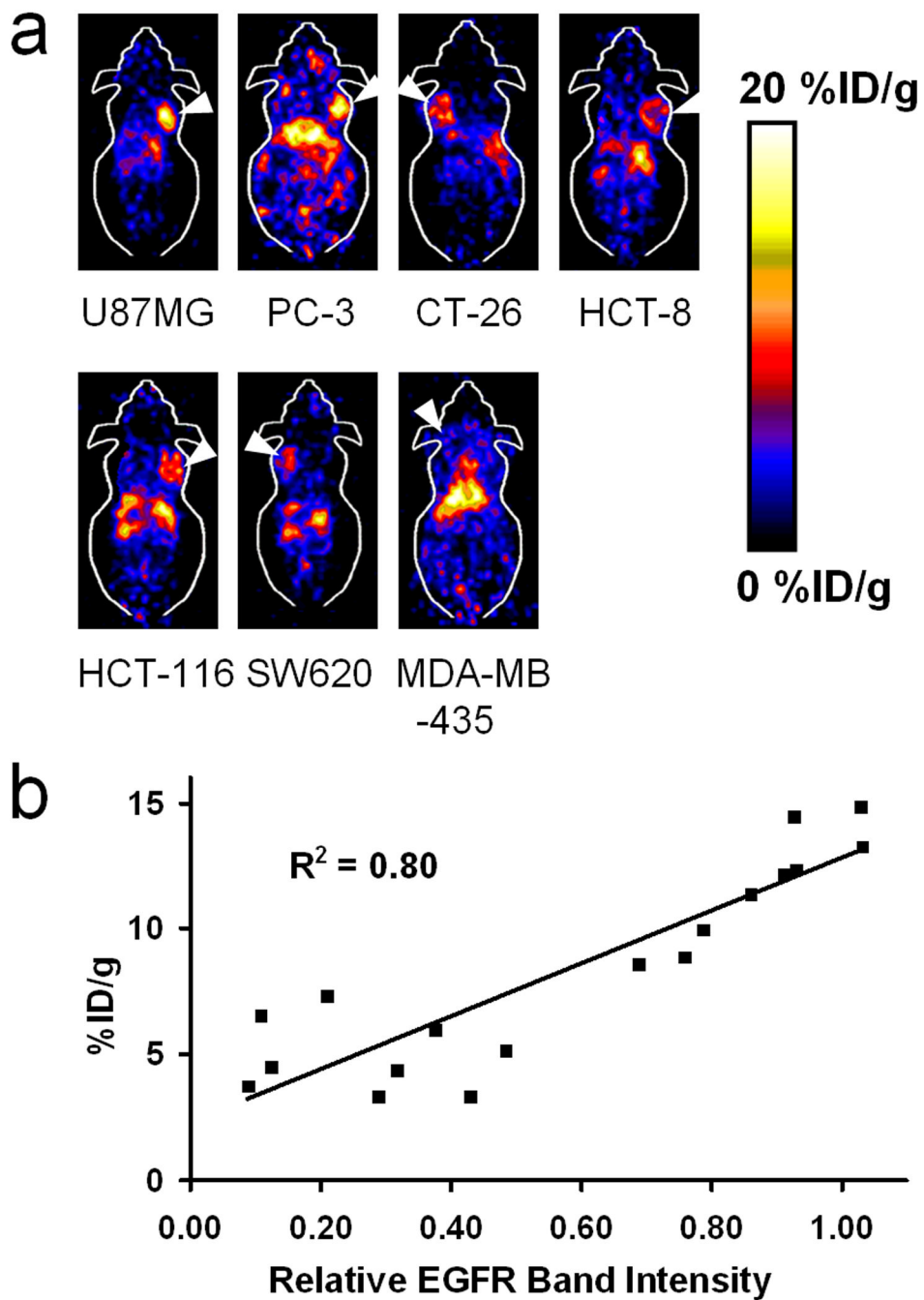
Fig. 7.
Quantitative PET imaging of EGFR expression in various tumor models including PCa. (**a**) Small-animal PET images of seven xenograft tumor models at 48 hours post-injection of ^{64}Cu-DOTA-cetuximab. Decay-corrected whole body coronal images are shown and the tumors are indicated by arrowheads. (**b**) Correlation of EGFR expression level (measured by Western blotting) and the %ID/g values (measured by microPET scans) of different tumors at 48 hours post-injection. Adapted from (Cai et al. 2007a)

Fig. 8.
PET imaging of PSCA expression with engineered antibody fragments. (**a**) Serial coronal small-animal PET projections of a mouse bearing a PCa xenograft (indicated by "+") injected with a ^{124}I-labeled anti-PSCA minibody. B: bladder. (**b**) Serial coronal small-animal PET images of PCa tumor-bearing mice after administration of a ^{124}I-labeled anti-PSCA diabody. +: PSCA-positive tumor;−: PSCA-negative tumor. Adapted from (Leyton et al. 2008a; Leyton et al. 2008b)